Journal of
Applied and Computational Mechanics

Investigation of Nanofluid Natural Convection Heat Transfer in Open Ended L-shaped Cavities utilizing LBM

Hasan Mohammadifar[1], Hasan Sajjadi[2], Mohammad Rahnama[1], Saeed Jafari[1], Yan Wang[3]

[1] Department of Mechanical Engineering, Shahid Bahonar University of Kerman
Kerman, P.O. Box 76175-133, Iran, Emails: hasan4219@gmail.com, rahnama@uk.ac.ir, jafari@uk.ac.ir

[2] Department of Mechanical Engineering, University of Bojnord, Bojnord, P.C. 945 3155111, Iran, Emails: hsajjadi@clarkson.edu, hasansajjadi@gmail.com

[3] Department of Aerodynamics, Nanjing University of Aeronautics and Astronautics, Nanjing, China, Email: aerowangy@nuaa.edu.cn

Abstract. In this paper, laminar natural convection of copper/water nanofluid in an open-ended L-shaped cavity is investigated by Lattice Boltzmann Model (LBM). The results are compared by previous studies that are in good agreement. Influences of Rayleigh number (Ra = 10^3, 10^4, 10^5, 10^6), cavity aspect ratio (AR = 0.2, 0.4, 0.6) and volume concentration of Cu nanoparticles ($0 \leq \phi \leq 0.1$) on the momentum, thermal fields and heat transfer in the enclosure are studied. Also, the effect of changing the boundary conditions, on the heat transfer rate has been investigated. It is observed that maximum heat transfer enhancement by adding the nanoparticles for Ra = 10^6 with AR = 0.4 (32.76%) occurs. Results illustrate that increasing the cavity aspect ratio decreases heat transfer rate for Ra = 10^3 and Ra = 10^4. The least and most heat transfer rate for Ra = 10^5 occurs in enclosures by aspect ratios of 0.2 and 0.4 respectively, while it was observed at Ra = 10^6 for minimum and maximum rate of heat transfer the opposite behavior that at Ra = 10^5 occurs.

Keywords: Lattice Boltzmann method, Natural convection, Nanofluid, Open-ended L-shaped cavity, Aspect ratio.

1. Introduction

The study of various types of convective heat transfer, which is one of the most important and practical mechanisms of heat and energy transfer in many engineering applications in industry, has long been considered by scientists [1-4]. In recent years, many researchers have investigated free convection heat transfer by Lattice Boltzmann method (LBM) [5-7]. Implementation of LBM results in more efficient computations in complex geometries and multi-component flows compared to other computational fluid dynamics (CFD) common methods [8-14]. The combination of a fluid with nanometer-sized particles (nanoparticles) is called nanofluid that first was introduced by Choi [15]. Then, many studies were done on the types of heat transfer in the presence of nanofluids, which can be referred to as recent works such as; Hashim et al. [16], Carrillo-Berdugo et al. [17] and Sheikholeslami et al. [18]. Chamkha et al. [19] reviewed all works that were studied by numerical, analytical, and experimental on the effect of nanofluids on fluid flow and heat transfer in microchannels. Also Chamkha et al. [20] numerically analyzed magnetohydrodynamic (MHD) mixed convective heat transfer of a nanofluid in a lid-driven porous cavity with a heat source and heat sink located at the bottom and upper wall respectively, Also after that, Rashad et al. [21] investigated the same study for natural convection.

The first research on natural convection thermal flow in a cavity containing nanofluids was performed by Khanafer et al. [22]. They showed that with increasing nanoparticles volume fraction for all Grashof numbers considered, heat transfer rate enhances. Afterward, many researchers investigated natural convection in cavities contains nanofluids [23-37]. They performed the effects of various parameters such as; Ra number, aspect ratio (AR) and inclination angles of cavities, and several types of nanoparticles with water as the base fluid of nanofluid. Some researchers have focused on the free convection heat transfer in an enclosure with inner hot or cold obstacles or fins [38-43]. Chamkha et al. [44] used the Galerkin finite element method (FEM) to solve the melting process of a phase change material on the free convection thermal flow in an enclosure containing single and hybrid nanofluid with a heated inner cylinder. Their results conducted that by increment Fourier number the melting rate first increases and then decreases. Hajatzadeh et al. [45] by finite volume method (FVM) explored free convection flow in a square cavity containing Al_2O_3/Water nanofluid and with two isothermal obstacles and sinusoidal boundary conditions with applying Magnetohydrodynamic. Their results demonstrate that the heat transfer decreased by augmenting aspect ratio. Siavashi et al. [46] used FVM to simulate free convection in a cavity containing copper-water nanofluid with an array of porous fins. They demonstrated that a high volume concentration of nanoparticles enhances the heat transfer less than the low volume concentration of nanoparticles. Moreover, the entropy generation declines by adding more fins. The LBM was used by Vijaybabu

and Dhinakaran [47] to investigate MHD free convection flow and heat transfer of H_2O/Al_2O_3 nanofluid between a heated porous triangular-shaped and cold square cavity. They found that the effect of heat transfer decrement due to increment in Hartmann number (Ha) is eminent for higher Darcy number. Hashim et al. [48] numerically solved free convection thermal flow in a wavy-walled including H_2O/Al_2O_3 nanofluid with a heated block in the center and heated the bottom wall. They concluded that with increment the size of each side of the heated block, the heat transfer rate increases for all concentrations of the nanoparticles. Rafie and Payan [49] examined the effect of various parameters including the most favorable position and length of a thick fin at the two inclination of the fin on the vertical hot wall of a square cavity. Their results showed that a thick fin with grooves and an obliquely thin fin have a better decrement heat transfer rate than a direct thick fin at Ra=10^4 and Ra=10^6 respectively.

A number of recent researches have been done on free convection in the curve and non-quadrilateral geometries, among them, are those related to buildings ventilation, solar-collectors, cooling systems of electronic equipment, the molten core of the Earth, etc [50-54]. Parvin et al. [55] applied FEM to simulation free convection in an annulus including H_2O/Al_2O_3 nanofluid. They are applied two thermal conductivity models to measure the heat transfer increment in the annulus. Sheikholeslami et al. [56] applied LBM to simulate the Cu/water nanofluid natural convection thermal flow in a square cavity with curve boundaries. They concluded that flow and thermal fields strongly depend on the inclination angle of the cavity. Zare Ghadi et al. [57] analyzed double-diffusive free convection fluid flow and heat transfer inside a curved enclosure including a porous media by FVM. They scrutinized the effects of disparate parameters on the velocity and temperature fields and heat transfer. Jayhooni and Jafarpur [58] solved laminar free convection flow and heat transfer around the bi-sphere, cylinder, prolate, and cylinder with hemispherical ends numerically. They found that mean Nusselt numbers based on the square surface area are independent of the geometries for the Ra numbers with laminar flow. The FVM was applied by Rezvani et al. [59] to carry out entropy generation for free convection in cylindrical cavities. They showed that decreasing the irreversibility ratio decreases the total entropy generation. Ghasemi and Aminossadati [60] numerically studied free convection inside a right triangular cavity that contains nanofluid. They demonstrated that the highest heat transfer rate occurs in high Ra numbers in an optimal amount of the volume fraction of the nanoparticles. Saleh et al. [61] simulated natural convection thermal flow inside a trapezoidal enclosure with utilizing nanofluid. They discovered the relevance for medium Nusselt number as a function of the gradient wall's angel, Grashof number, effective thermal conductivity, and viscidity. Natural convection in an inclined triangular enclosure containing water utilizing LBM was done by Mejri et al. [62]. Their results indicated that the gradient angle effect on heat transfer rate augments with increment Ra number. Chamkha et al. [63] by FVM (SIMPLE) solved MHD free convective heat transfer in a C-Shaped enclosure filled with CuO-water nanofluid. They found that the magnetic field causes a reduction quickly the entropy generation rate. Mohebbi et al. [64] utilized LBM to investigate the effect of the location of the heat source on free convection flow in a C-shaped cavity filled with nanofluid. They showed that increment in the Nusselt number of the nanofluid at low Rayleigh numbers is independent of the location of the heat source. Bondareva et al. [65] examined laminar natural convection heat transfer in a partially heated open triangular enclosure contain Cu/H_2O nanofluid applying finite difference method (FDM). They obtained results which demonstrated increasing heat transfer with nanoparticles volume fraction occurs chiefly for high Ra number. Mahmoodi et al. [66] and Mansour et al. [67] solved free convection inside C-shaped and T-shaped cavities including Copper/water nanofluid respectively. They acquired that the rate of heat transfer enhances with reducing the aspect ratio of the enclosure. Bakier [68] numerically studied free convection thermal heat transfer in segmentally C-shape open-ended cavity containing nanofluid. Their results highlighted that at a low Ra number, the heat and mass transfer rates through the opening boundaries enhance in the presence of nanoparticles. FVM was employed by Hemmat Esfea et al. [69] to solve free convection thermal flow inside T-shaped cavities including (MWCNT-COOH)/H_2O nanofluids. They concluded that increment in aspect ratio reduces the mean Nusselt number. Mahmud [70] and Tasnim and Mahmud [71] were among the first researchers who started their simulation on free convection inside L-shaped enclosures containing air. Afterward, Mahmoodi [72] numerically studied the free convection flow of Cu/H_2O nanofluid in L-shaped cavities. He obtained a mean Nusselt number for all ranges of cavity aspect ratio that enhances with an increment in the Ra and volume concentration of the nanoparticles. Moreover, he illustrated that the heat transfer rate increases by reducing the aspect ratio of the cavity. Sheikholeslami et al. [73] analyzed the effects of different parameters on natural convection in an inclined L-shape enclosure containing Cu/H_2O nanofluid. They showed that minimum and maximum mean Nusselt number corresponds to 45° and -45°, respectively for Ra=10^4, in the event that an opposite result is observed for Ra=10^5. Mliki et al. [74] numerically studied natural convection in the L-shaped cavity including Cu/H_2O nanofluid by LBM. They concluded that the existence of nanofluid causes mean Nusselt number to increase. They also showed that reducing the aspect ratio increases the mean Nusselt number. Mohebbi and Rashidi [75] studied free convection thermal flow numerically in an L-shaped cavity contain Al_2O_3/H_2O nanofluid and an internal heating obstacle using LBM. They concluded that with decreasing nanoparticle diameter and aspect ratio of the channel and the increasing Ra and height of the obstacle the heat transfer enhances. Rahimi et al. [76] utilized LBM to study natural convection in a hollow L-shaped cavity filled with hybrid nanofluid. Thermophysical properties of SiO_2-TiO_2/water-Ethylene glycol hybrid nanofluid are obtained experimentally. They demonstrated that the total entropy generation reduces with increasing of the volume concentration of the nanoparticles. Zhang et al. [77] used the finite difference lattice Boltzmann model (FDLBM) to analyze entropy distributions on the MHD natural convection thermal flow in an L-shaped enclosure filled with several types of Newtonian and non-Newtonian fluids. They concluded that the heat transfer and total entropy generation decreases by increasing Rayleigh and Hartmann numbers, in addition, the dependency rate of changes in heat transfer and total entropy generation to the Ha number and Ra number increases with the decrement power-law index. Izadi et al. [78] numerically studied the effect of disparate important parameters considered in relation to the MHD flow and porosity, on MHD free convection inside a porous enclosure. They discovered that at a low Ra number heat transfer enhances with an increment strength ratio of the two magnetic sources and magnetic number. The LBM was used by Abbassi et al. [79] to simulate MHD natural convection thermal flow inside an incinerator shaped cavity filled by Al_2O_3-H_2O nanofluid with a heated obstacle placed on the bottom wall. They demonstrated that minimum entropy generation and maximum heat transfer in incinerator inclination angle 270° and 90° occurs. Yuan Ma et al. [80] used LBM to investigate the free convection in a U-shaped enclosure containing Al_2O_3-H_2O or TiO_2-H_2O nanofluid and including a heated block. They obtained results showed that by increment the U-shaped cavity's aspect ratio, the mean Nusselt number enhanced. Seo et al. [81] performed 3-D natural convection thermal flow inside a cavity including a hot, circular cylinder or an elliptical cylinder. They found that the heat transfer rate is dependent on the radius variation for the circular or elliptical cylinders. Dutta et al. [82] examined the efficacy of various parameters on the free convection thermal flow and entropy generation in a rhombic cavity containing Cu/H_2O nanofluids under the influence of magnetohydrodynamics. They reported that by increasing Hartmann number for all range of the Ra number and inclination angles of the cavity the total entropy generation rate declines. The LBM investigation of MHD free convection in a V-shaped electronic device including Cu-H_2O nanofluid has been studied by Purusothaman and Hasani [83]. They exhibited that the heat transfer reduces with enhancement of the aspect ratio and Ha. Moreover, the Optimum inclination angle is 45 for maximum heat flow rate. Yahiaoui et al. [84] numerically (FVM) examined free convection thermal flow inside the square cavity and cavities with concave and convex constant temperature walls utilizing copper-water nanofluid. They discovered that

the heat transfer in a square cavity was more than the other cavities with concave and convex walls. Almeshaal et al. [85] carried out Rayleigh-Bénard free convection thermal flow by FVM and experimental thermophysical properties of the (MWCNT)-water nanofluid inside the three-dimensional L-shaped cavity filled. They realized that in AR=0.4 the highest heat transfer occurs for Ra<10^5 and volume concentration of the nanoparticles less than 0.03. Dogonchi et al. [86] studied the natural convective of Cu-H_2O nanofluid inside the circular cavity including porous interior heat source. They formulated a new correlation for the mean Nu number by the effect Nanoparticles volume concentration, viscous dissipation, and Ra number.

As we know, heat transfer is improved by changing the flow geometry, boundary conditions, adding secondary surfaces (such as fins), changing the behavior of the flow, and changing the fluid properties. Therefore the major aims of this work are to perceive the ability of the LBM in investigating the behavior of nanofluid in complicated geometries and boundaries and also enhancing the rate of heat transfer by changing the flow geometry, boundary conditions, and adding nanoparticles. So, the D2Q9 model is used to solve the temperature and velocity field of the laminar natural convection of Cu-H_2O nanofluid in open-ended L-shaped cavities. In addition in order to solve the problem more accurately the unknown density and internal energy distribution functions can be calculated by a second-order approximation. The effects of various parameters such as; Ra, volume concentration, and various aspect ratios on the heat transfer have been considered. And finally, to investigate the effect of changing the boundary conditions, on the heat transfer rate, the present study has been compared with the work of Mahmoodi [72] for base fluid and nanofluid.

2. Mathematical formulation

2.1. Problem statement

As it is shown in Fig. 1, in the current work, an open-ended L-shaped cavity is considered. The dimensionless temperature of the L shaped right and left walls are fixed at θ_c and θ_h respectively, and the top wall is adiabatic. From the east opening boundary, Cu-water nanofluid with a constant temperature (θ_c) enters into the open-ended L-shaped cavity. The height and width of the open-ended L-shaped cavity are shown by Z. The aspect ratio (AR=D/Z) of the enclosure is described as the ratio of thickness divided by the height or width of the enclosure. The size of the length of the perpendicular to the plane of the enclosure supposed to be long enough; therefore, the problem is assumed as 2-dimensions. The thermophysical properties of copper nanoparticles and water are shown in Table 1. Several assumptions for Cu-H_2O nanofluid have been proposed as follows: between water and copper nanoparticles, not existence any slip and are in thermal equilibrium. The Newtonian nanofluid flow is supposed to be incompressible and laminar. The nanofluid density changes are calculated by Boussinesq approximation [87]. Therefore for the current study, the Navier-Stokes and energy equations in the non-dimensional state are derived as follows [72]:

$$\frac{\partial U}{\partial X} + \frac{\partial V}{\partial Y} = 0 \tag{1}$$

$$U\frac{\partial U}{\partial X} + V\frac{\partial U}{\partial Y} = -\frac{\partial P}{\partial X} + \mathrm{Pr}_{nf}\left(\frac{\partial^2 U}{\partial X^2} + \frac{\partial^2 U}{\partial Y^2}\right) \tag{2}$$

$$U\frac{\partial V}{\partial X} + V\frac{\partial V}{\partial Y} = -\frac{\partial P}{\partial Y} + \mathrm{Pr}_{nf}\left(\frac{\partial^2 V}{\partial X^2} + \frac{\partial^2 V}{\partial Y^2}\right) + Ra_{nf}\,\mathrm{Pr}_{nf}\,\theta \tag{3}$$

$$U\frac{\partial \theta}{\partial X} + V\frac{\partial \theta}{\partial Y} = \left(\frac{\partial^2 \theta}{\partial X^2} + \frac{\partial^2 \theta}{\partial Y^2}\right) \tag{4}$$

where the non-dimensional parameters are defined as follows:

$$X = \frac{x}{Z},\ Y = \frac{y}{Z},\ U = \frac{uZ}{\alpha_{nf}},\ V = \frac{vZ}{\alpha_{nf}},\ \theta = \frac{T - T_c}{T_h - T_c},\ P = \frac{pZ^2}{\rho_{nf}\alpha_{nf}^2},\ \mathrm{Pr}_{nf} = \frac{\vartheta_{nf}}{\alpha_{nf}},\ Ra_{nf} = \frac{g\beta_{nf}\left(T_h - T_C\right)Z^3}{\alpha_{nf}\vartheta_{nf}} \tag{5}$$
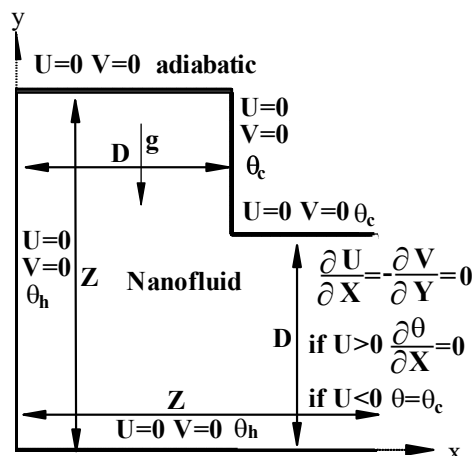

Fig. 1. Geometry of the open-ended L-shaped cavity considered in the present study.

Table 1. Thermophysical properties.

Physical properties	Water	Cu
$C_p \, (J/kg\,K)$	4179	385
$\rho \, (kg/m^3)$	997.1	8933
$k \, (W/m\,K)$	0.613	400
$\beta \, (K^{-1})$	21×10^{-5}	1.67×10^{-5}
$\alpha \, (m^2/s)$	1.471×10^{-7}	-
$\mu \, (kg/m\,s)$	8.55×10^{-4}	-

2.2. Lattice Boltzmann method for natural convection simulation

For simulation, the incompressible fluid flow and heat transfer topics, LBM uses two distribution functions g and f for the temperature and velocity fields, respectively [88].

$$f_i\left(x + c_i \Delta t, t + \Delta t\right) - f_i\left(x,t\right) = -\frac{1}{\tau_v}\left[f_i\left(x,t\right) - f_i^{eq}\left(x,t\right)\right] + \Delta t F_i \tag{6}$$

$$g_i\left(x + c_i \Delta t, t + \Delta t\right) - g_i\left(x,t\right) = -\frac{1}{\tau_c}\left[g_i\left(x,t\right) - g_i^{eq}\left(x,t\right)\right] \tag{7}$$

where ⬚t is indicative of lattice time step and is equal to 1. F is defined as the external force. τ_c, τ_v is the relaxation time for the temperature and velocity fields, respectively.

In this study, the nine-velocity two-dimensional (D2Q9) model (Fig. 2a) is used for temperature and velocity field, so the weighting factors (ω_i) and the discrete particle velocity vectors (c_i) are obtained in the following equations:

$$\omega_i = \begin{cases} 4/9 & i = 0 \\ 1/9 & i = 1 - 4 \\ 1/36 & i = 5 - 8 \end{cases} \tag{8}$$

$$c_i = \begin{cases} 0 & i = 0 \\ c\left(\cos\left[(i-1)\pi/2\right], \sin\left[(i-1)\pi/2\right]\right) & i = 1 - 4 \\ c\sqrt{2}\left(\cos\left[(i-5)\pi/2 + \pi/4\right], \sin\left[(i-5)\pi/2 + \pi/4\right]\right) & i = 5 - 8 \end{cases} \tag{9}$$

g_i^{eq}, f_i^{eq} are the equilibrium distribution functions that have a proper determined functional dependency on the local hydrodynamic properties which are computed with Eqs. (10) and (11) for velocity and temperature fields respectively.

$$f_i^{eq}\left(x,t\right) = \omega_i\,\rho\left[1 + 3\frac{c_i.u}{c^2} + \frac{9}{2}\frac{\left(c_i.u\right)^2}{c^4} - \frac{3}{2}\frac{u.u}{c^2}\right] \tag{10}$$

$$g_i^{eq}\left(x,t\right) = \omega_i\,\theta\left[1 + 3\frac{c_i.u}{c^2}\right] \tag{11}$$

ρ and u are defined as the macroscopic density and velocity, respectively, c is defined as the lattice speed and equals to $\Delta x/\Delta t = 1$ where ⬚x is defined as lattice space.
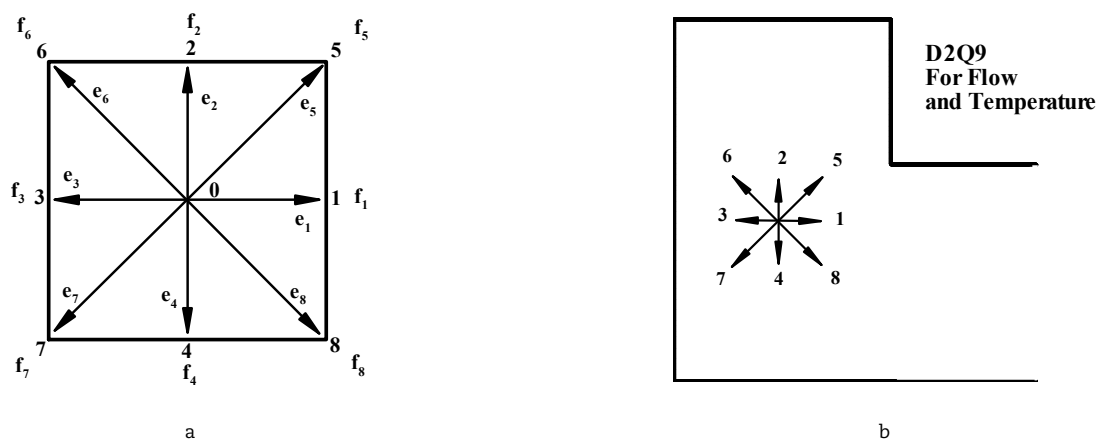

Fig. 2. (a) The discrete velocity vectors for D2Q9. (b) Domain boundaries.

The thermal diffusivity (α) and kinematic viscosity (ϑ) are defined by the τ_c, τ_ν in the following format:

$$\vartheta = \left[\tau_\nu - \frac{1}{2}\right]c_s^2\Delta t \qquad \text{and} \qquad \alpha = \left[\tau_c - \frac{1}{2}\right]c_s^2\Delta t \tag{12}$$

where $c_s = c/\sqrt{3}$ is defined as the lattice speed of sound.

External force (F) calculated as follows:

$$F = 3\omega_i g_y \beta \Delta\theta \tag{13}$$

where $\boxtimes \theta$ is equal to (θ-θ_m) whereas $\theta_m = (\theta_h + \theta_c)/2$ and β is the thermal expansion coefficient.

Eventually, ρ, u, θ can be calculated with the following equations.

$$\text{Flow density:} \quad \rho(x,t) = \sum_i f_i(x,t) \tag{14}$$

$$\text{Momentum:} \quad \rho u(x,t) = \sum_i f_i(x,t)c_i \tag{15}$$

$$\text{Temperature:} \quad \theta = \sum_i g_i(x,t) \tag{16}$$

2.3. Boundary conditions for flow field

At the boundary nodes the unknown distribution functions mentioned to the fluid zone must be determined (Fig. 2 b). Bounce back boundary condition is applied on the no-slip solid boundaries. At the open boundary the unknown density distribution functions can be defined by a second-order approximation:

$$f_{6,n} = \frac{4}{3}f_{6,n-1} - \frac{1}{3}f_{6,n-2}$$
$$f_{7,n} = \frac{4}{3}f_{7,n-1} - \frac{1}{3}f_{7,n-2} \tag{17}$$
$$f_{3,n} = \frac{4}{3}f_{3,n-1} - \frac{1}{3}f_{3,n-2}$$

2.4. Boundary conditions for temperature field

The north boundary kept adiabatic and bounce back boundary condition can be applied to it. The temperature boundary condition at the open boundary is known so that for input flow to the enclosure $\theta_c = 0.0$ and for output flow from the enclosure is adiabatic. Temperatures are defined in the west of L-shaped wall $\theta_h = 1.0$ and in the east of L-shaped wall $\theta_c = 0.0$. In this study D2Q9 is used for the unknown internal energy distribution function at the open boundary, east and west boundaries that can be acquired by the following equations [89]:

For the west L-shaped wall (on the hot walls)

$$\begin{cases} g_1 = \theta_h(\omega_1 + \omega_3) - g_3 \\ g_5 = \theta_h(\omega_5 + \omega_7) - g_7 \quad \text{on the vertical walls} \\ g_8 = \theta_h(\omega_8 + \omega_6) - g_6 \end{cases}$$

$$\tag{18}$$

$$\begin{cases} g_2 = \theta_h(\omega_2 + \omega_4) - g_4 \\ g_5 = \theta_h(\omega_5 + \omega_7) - g_7 \quad \text{on the horizontal walls} \\ g_6 = \theta_h(\omega_6 + \omega_8) - g_8 \end{cases}$$

For the east L-shaped wall (on the cold walls)

$$g_3 = 0 - g_1, \ g_7 = 0 - g_5, \ g_6 = 0 - g_8 \quad \text{on the vertical walls}$$

$$g_4 = 0 - g_2, \ g_7 = 0 - g_5, \ g_8 = 0 - g_6 \quad \text{on the horizontal walls} \tag{19}$$

For the east open boundary (by a second-order approximation)

$$\text{If } u < 0 \text{ then}: \ g_3 = 0 - g_1, \ g_7 = 0 - g_5, \ g_6 = 0 - g_8$$

$$g_{6,n} = \frac{4}{3}g_{6,n-1} - \frac{1}{3}g_{6,n-2} \tag{20a}$$

$$\text{If } u > 0 \text{ then}: \ g_{7,n} = \frac{4}{3}g_{7,n-1} - \frac{1}{3}g_{7,n-2}$$

$$g_{3,n} = \frac{4}{3}g_{3,n-1} - \frac{1}{3}g_{3,n-2} \tag{20b}$$

2.5. Method of solution

With keeping constant Ra number, Mach number and Prandtl number (Pr) the thermal diffusivity and viscosity are computed from the following formula:

$$v = \sqrt{\frac{Ma^2 m^2 \Pr c^2}{Ra}} \tag{21}$$

where m is the number of lattices in X and Y directions. Pr and Ra numbers are described as $Pr = \vartheta/\alpha$ and $Ra = (\beta g_y Z^3 (T_h - T_c))/\vartheta\alpha$, respectively. Mach number should be less than $Ma = 0.3$ for an incompressible flow [29]. The viscosity and subsequently thermal diffusivity can be computed by Eq. (21). Eventually with Eq. (12) can be calculated the relaxation times for temperature and flow distribution functions.

2.6. Lattice Boltzmann method for nanofluid

In this study, important control parameters are the Ra number with Pr number. The nanofluid is assumed to be like a pure fluid and then nanofluid qualities are obtained that are practical for the governing equations. The nanofluid density changes in the buoyant force are calculated by Boussinesq approximation. The relevant thermophysical properties are shown in Table 1.

The effective density of a nanofluid can be calculated by [90]:

$$\rho_{nf} = (1 - \varphi)\rho_f + \varphi\rho_s \tag{22}$$

where $(\rho c_p)_{nf}$ is as the heat capacity and the thermal expansion coefficient of the nanofluid are obtained as [91]:

$$(\rho c_p)_{nf} = (1 - \varphi)(\rho c_p)_f + \varphi(\rho c_p)_s \tag{23}$$

$$(\rho\beta)_{nf} = (1 - \varphi)(\rho\beta)_f + \varphi(\rho\beta)_s \tag{24}$$

where φ is being the volume concentration of the Cu nanoparticles. The effective dynamic viscosity of the Cu-water nanofluid can be computed with the Brinkman model [22] as the following equation.

$$\mu_{nf} = \frac{\mu_f}{(1 - \varphi)^{2.5}} \tag{25}$$

For computing effective thermal conductivity of the nanofluid is used the Maxwell-Garnetts model as regards the nanoparticles are assumed to be identical and spherical shapes [27]:

$$\frac{k_{nf}}{k_f} = \frac{k_s + 2k_f - 2\varphi(k_f - k_s)}{k_s + 2k_f + \varphi(k_f - k_s)} \tag{26}$$

Nusselt number is one of the basic non-dimensional parameters in the explanation of the free convection thermal flow mechanism. The local Nusselt number can be described as:

$$Nu_l = \frac{hZ}{k_f} \tag{27}$$

While the heat transfer coefficient can be written in the following formula:

$$h = \frac{q_w}{T_h - T_c} \tag{28}$$

The thermal conductivity is obtained as the following equations:

$$\begin{cases} k_{nf} = -\dfrac{q_w}{\partial T/\partial X} & \text{on the vertical walls} \\[2mm] k_{nf} = -\dfrac{q_w}{\partial T/\partial Y} & \text{on the horizontal walls} \end{cases} \tag{29}$$

By putting up Eqs. (28) and (29) in Eq. (27), the local Nusselt number for the vertical and horizontal parts of the L-shaped hot wall can be achieved in the following equations:

$$\begin{cases} Nu_l = -\left(\dfrac{k_{nf}}{k_f}\right)\dfrac{\partial \theta}{\partial X} & \text{on the vertical walls} \\[2mm] Nu_l = -\left(\dfrac{k_{nf}}{k_f}\right)\dfrac{\partial \theta}{\partial Y} & \text{on the horizontal walls} \end{cases} \tag{30}$$

Finally, the mean Nusselt number on the L-shaped hot wall can be achieved by the following formulation:

$$Nu = \frac{1}{2}\left(\int_0^1 Nu_l dX \big|_{Y=0} + \int_0^1 Nu_l dY \big|_{X=0}\right) \tag{31}$$

3. Code validation and grid independence

The convergence criterion is defined by the following phrase:

$$Error = \frac{\sum_{j=1}^{m}\sum_{i=1}^{n}\left|\lambda^{t+1} - \lambda^t\right|}{\sum_{j=1}^{m}\sum_{i=1}^{n}\left|\lambda^{t+1}\right|} \leq 10^{-7} \tag{32}$$
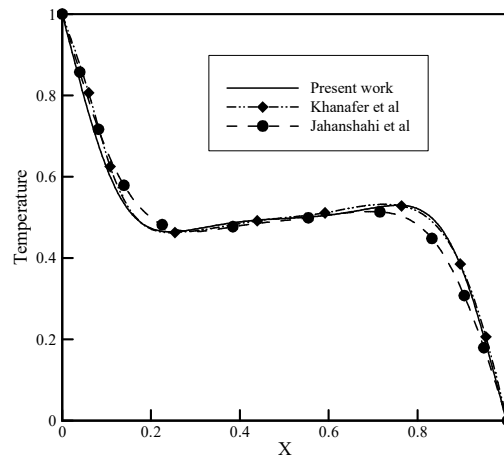
Fig. 3. Comparison of the temperature on axial midline between the present study, Khanafer et al. [22] and Jahanshahi et al. [27] $(Pr = 6.2, \varphi = 0.1, Gr = 10^4)$.
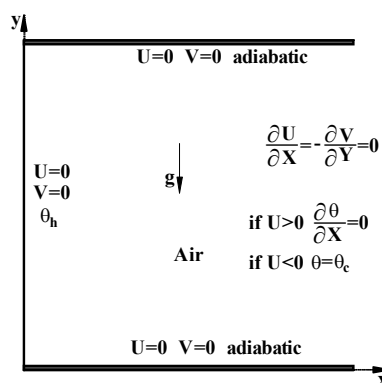

Fig. 4. Schematic view of the open-ended cavity considered in the previous investigations.
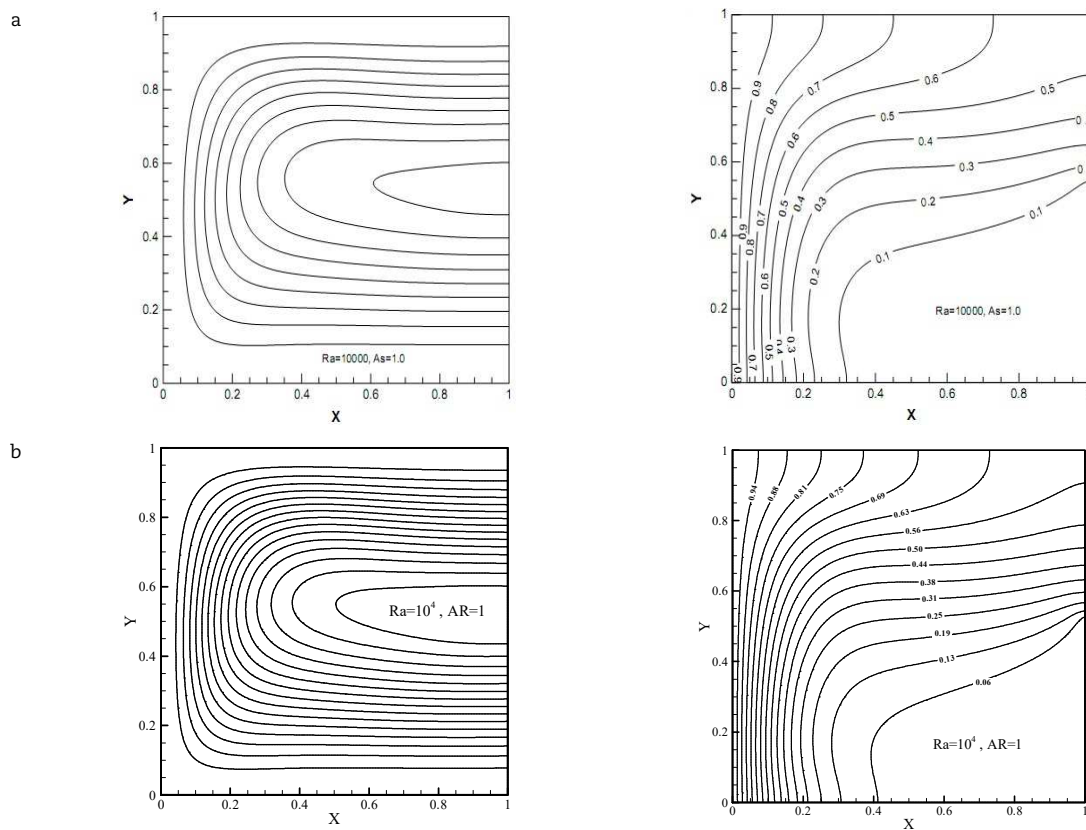

Fig. 5. Comparison of the streamlines (left) and isotherms (right) between (a) Mohamad et al. [89] and (b) the present study.

Table 2. Comparison of average Nusselt number on the hot wall for open-ended cavity.

Ra	Present study LBM D_2Q_9 , D_2Q_9	LBM [29] D_2Q_9 , D_2Q_4	LBM [89] D_2Q_9 , D_2Q_4	FVM [92]
10^4	3.275	3.319	3.377	3.264
10^5	7.263	7.391	7.323	7.261
10^6	14.355	14.404	14.380	14.076

Table 3. The average Nusselt number for L-shaped cavity contain air with AR = 0.25, comparisons of the present study with Mahmoodi [72] and Tasnim and Mahmud [71].

Ra	Present study (LBM)	Mahmoodi [72] (FVM)	Tasnim and Mahmud [71] (FVM)
10^3	3.277	3.270	3.251
10^4	3.290	3.259	3.255
10^5	3.829	3.855	3.903
10^6	9.050	9.340	9.331

where λ is a transport quantity. The numerical method has been used in this work is implemented in the FORTRAN program.

The current numerical study was already validated in three cases of this problem. For the first section, Fig. 3 shows a validation between the present study by LBM and outcomes of Khanafer et al. [22] and Jahanshahi et al. [27] for a cavity contain Cu-water nanofluid. For the second section, the stream functions and isotherms contour for an open-ended cavity with boundary conditions conforming to the Fig. 4 for air with Pr=0.71 of the current study were validated with the study of Mohamad et al. [89] in Fig. 5. Table 2, also displays the comparison of mean Nusselt number on the hot wall of the current work with studies of LBM by Mohammad et al. [89] and Kefayati et al. [29] and FVM by Mohammad et al. [92]. For the third section, the stream functions and isotherms contour for natural convection in L-shaped enclosure with AR=0.6 for net fluid (water) of the present simulation were compared with the results of Mahmoodi [72] in Fig. 7. Also, Table 3. indicates the comparison of mean Nusselt number on the hot wall of the free convection thermal flow in L-shaped enclosure contain air for AR=0.25 with boundary conditions conforming to the Fig. 6 of the present study (LBM) with studies of FVM by Mahmoodi [72] and Tasnim and Mahmud [71]. Therefore results of the current study have a good matching with prior works.
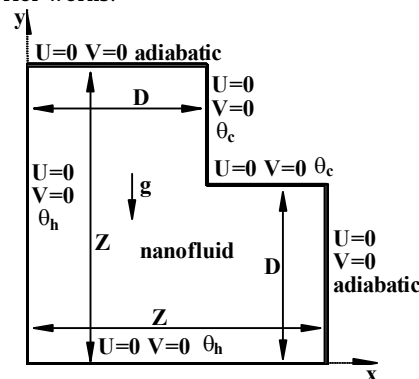
Fig. 6. Geometry of the L-shaped cavity considered in the previous investigations by Mostafa Mahmoodi [72].
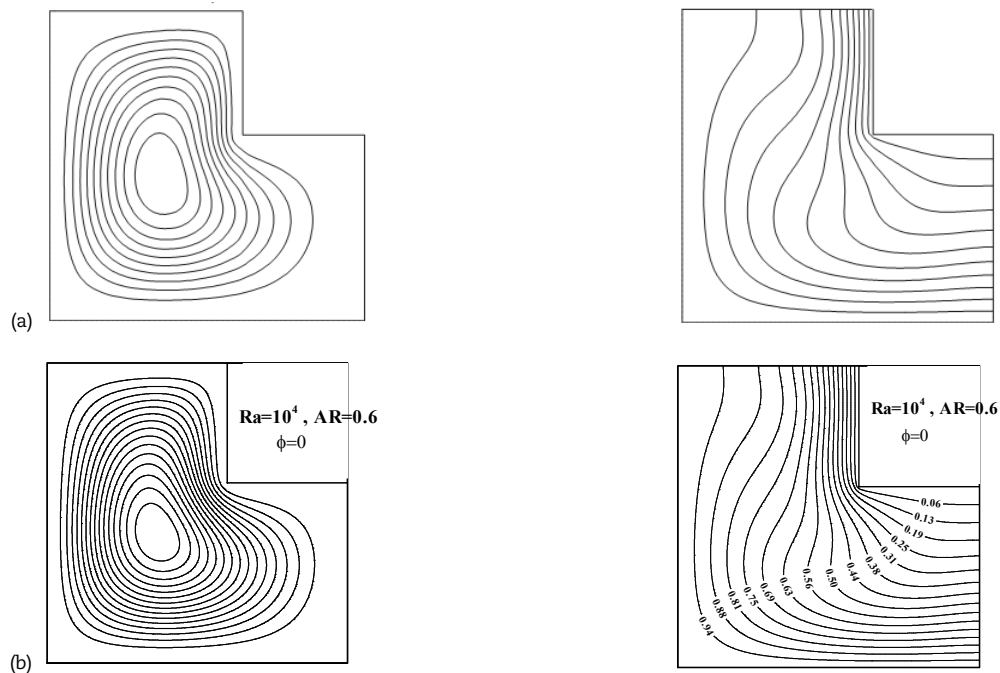
Fig. 7. Comparison of the streamlines and isotherms between (a) Mostafa Mahmoodi [72] and (b) the present study for Ra=10^4, AR=0.6, φ=0
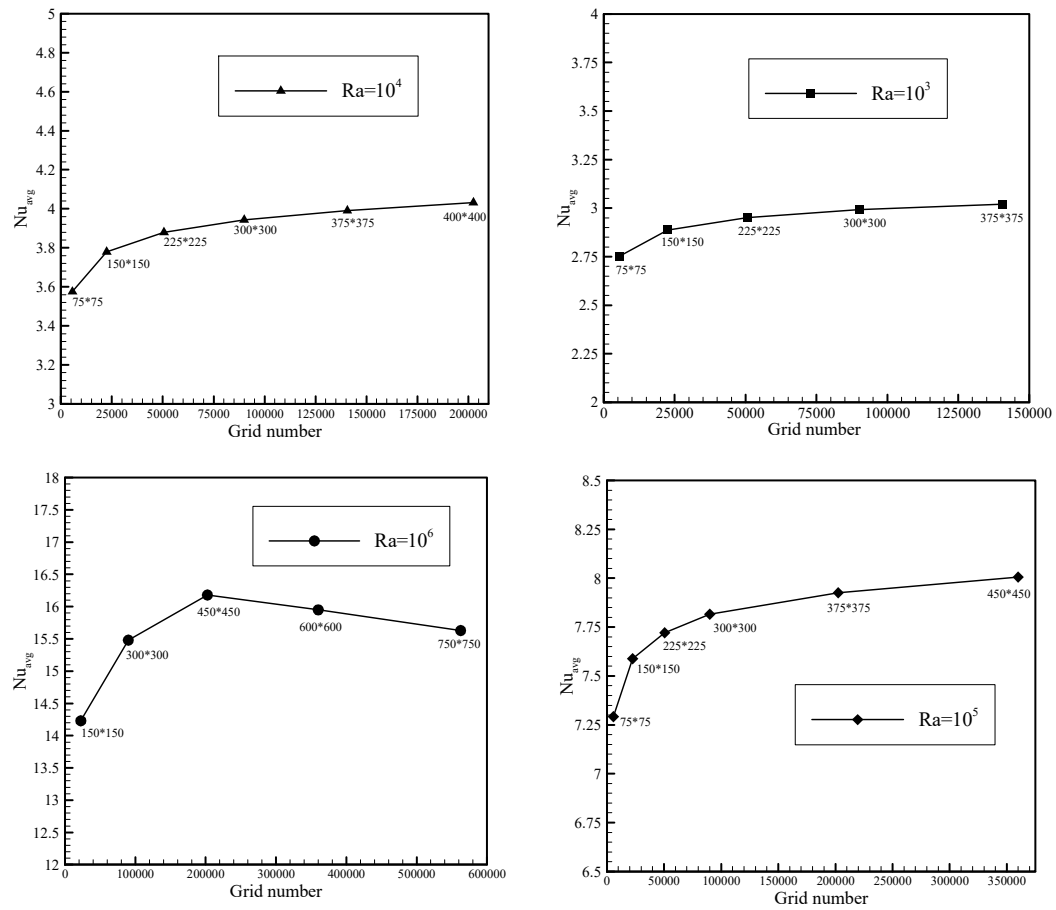
Fig. 8. Grid independence test: Nu_{avrage} versus grid number for $\varphi = 0.1$, $AR = 0.6$.
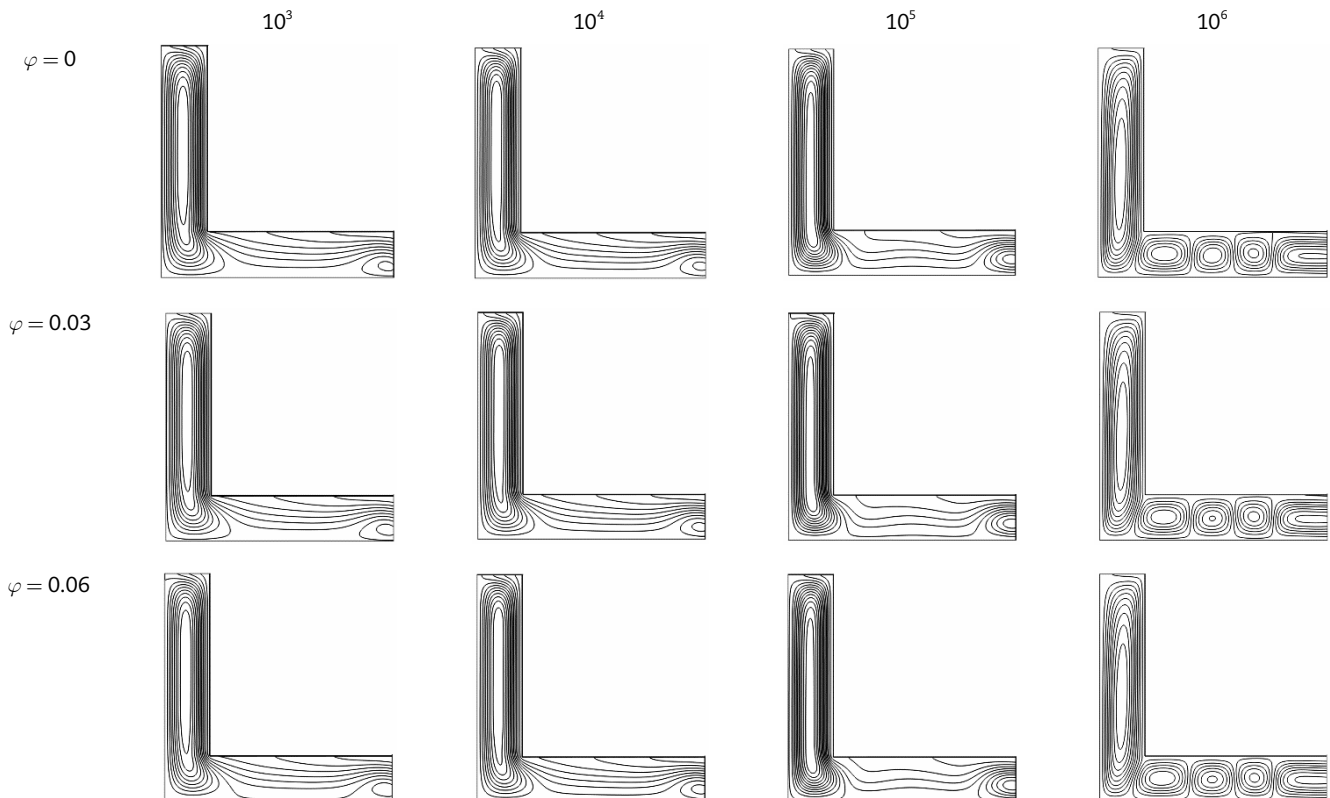

Fig. 9. Contour of the streamlines with volume fraction of the nanoparticles and Ra number for Cu/water nanofluid inside the Open-ended L-shaped cavity with AR=0.2.
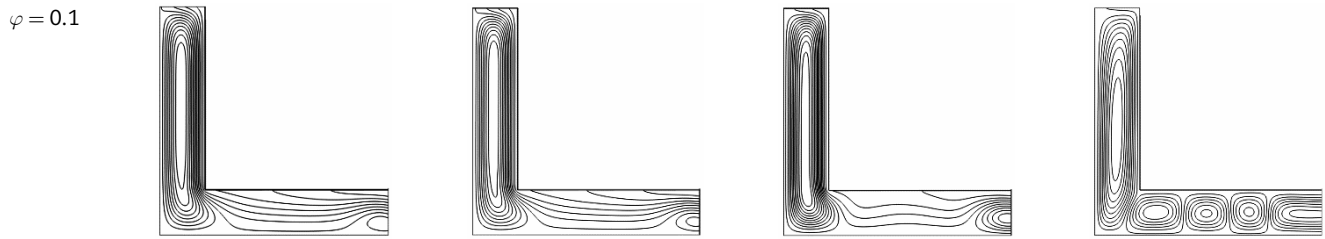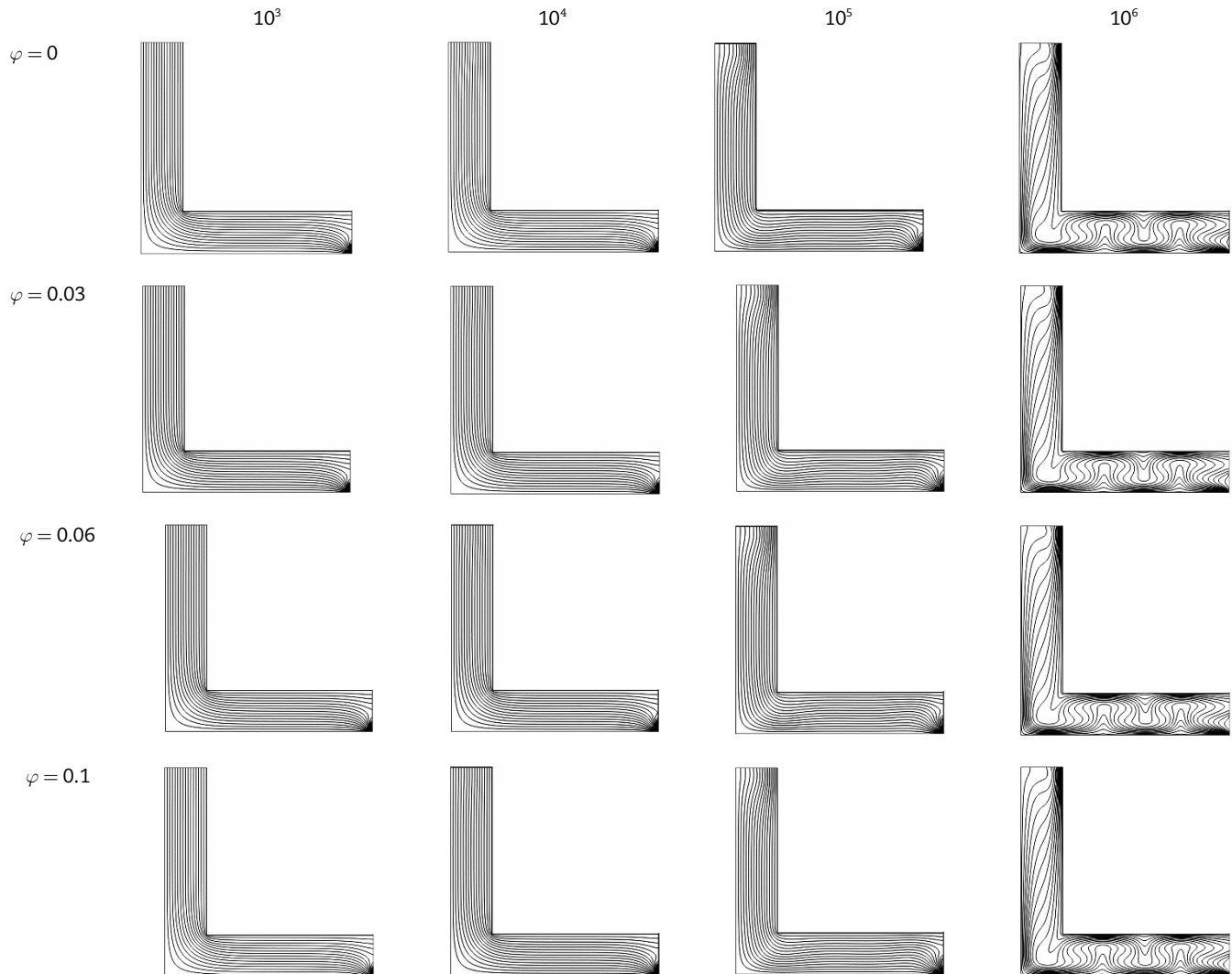
$\varphi = 0.1$

Fig. 9. Continued.

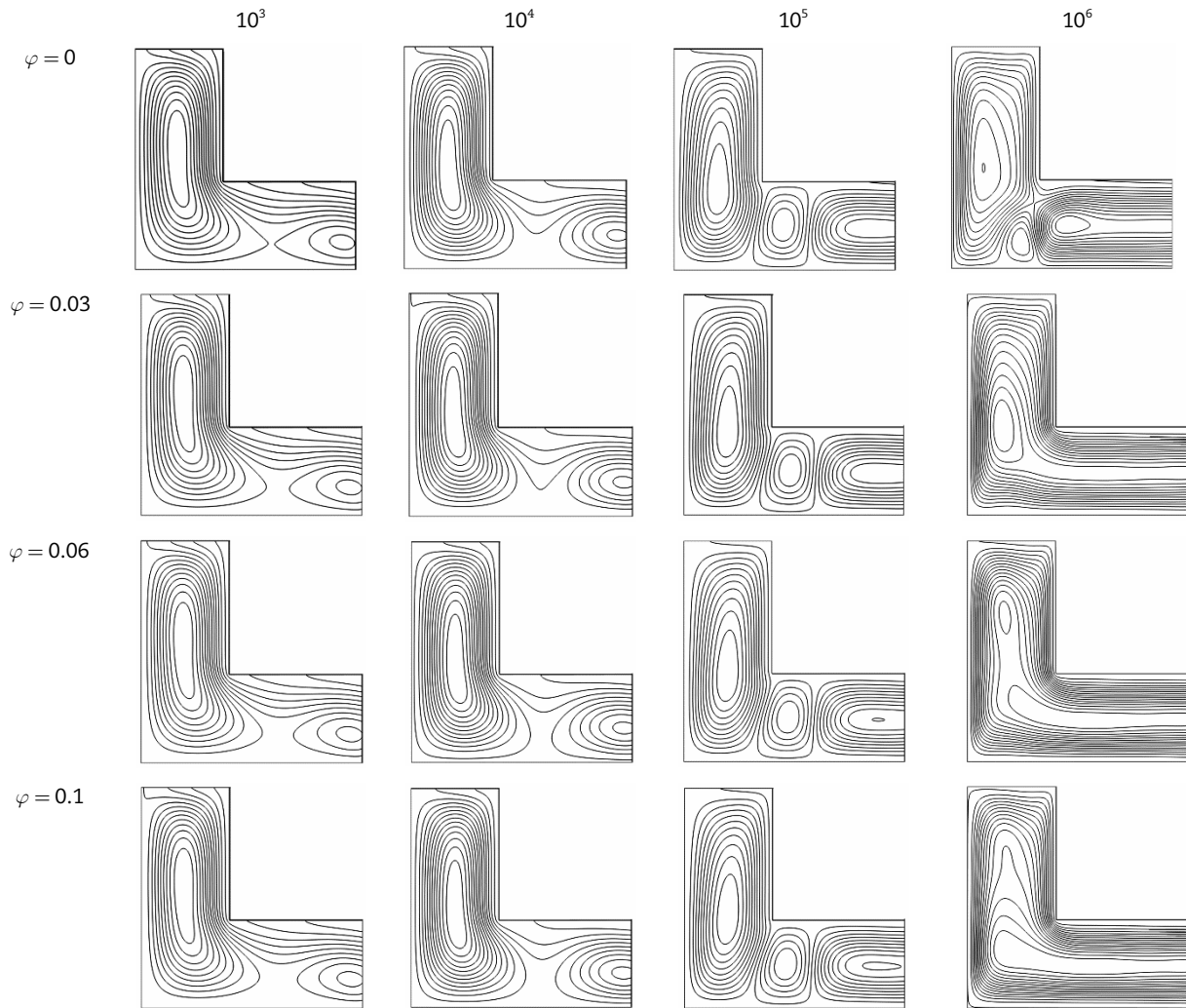| 10^3 | 10^4 | 10^5 | 10^6 |

$\varphi = 0$

$\varphi = 0.03$

$\varphi = 0.06$

$\varphi = 0.1$

Fig. 10. Contour of the isotherms with volume fraction of the nanoparticles and Ra number for Cu/water nanofluid inside the Open-ended L-shaped cavity with AR=0.2.

A grid independence check is performed for natural convection heat transfer in the open-ended L-shaped enclosure with aspect ratio 0.6 contain copper-water nanofluid with φ=0.1 for Ra numbers $10^3, 10^4, 10^5$ and 10^6. Several uniform grids are applied and for all of the grid sizes considered mean Nusselt number of the L-shaped hot wall is calculated. According to Fig. 8 the lattice sizes of 300×300, 375×375, 450×450 and 600×600 are chosen for Ra=$10^3, 10^4, 10^5$, and 10^6, respectively.

4. Results and discussion

In this part, numeric results for Cu/H_2O nanofluid natural convection in open-ended L-shaped cavities are reported. The influence of several parameters likes Ra number (10^3-10^6), the aspect ratio of the open-ended L-shaped cavity (0.2-0.6) and volume concentration of the nanoparticles (0-0.1) on the velocity and temperature fields were investigated.

Figs. 9 and 10 illustrate the effect of Ra and the volume concentration on temperature and flow distribution in the open-ended L-shaped cavity for AR=0.2. From the streamlines in Fig. 9 for aspect ratio 0.2 can be deduced a clockwise eddy is formed in the whole vertical part of the enclosure for all Ra number and volume concentration of solid particles. In the horizontal part of the L-shaped enclosure for Ra=10^6 for base fluid and nanofluid three eddies with rotating in the opposite direction are formed but for other Ra numbers, no eddy is formed. Also, streamlines model for all Ra numbers does not vary significantly when the concentration of the nanoparticles enhances. Fig. 10 shows that the isotherm lines for Ra=10^6 and all range of the concentration

of the nanoparticles are accumulated close to the walls in the vertical section and oscillating in the horizontal section of the L-shaped enclosure. But for other Ra numbers isotherm lines are parallel with walls of the enclosure for all range of the concentration of the nanoparticles that shows conduction is the prevail on the heat transfer mechanism. Therefore, at $Ra=10^6$, the isotherm lines vary considerably and heat transfer by convection thermal flow prevails. Also, it can be concluded that the effectiveness of nanoparticles on the open boundary region is insignificant.

Fig. 11. Contour of the streamlines with respect to the volume fraction of the nanoparticles and Ra number for Cu/water nanofluid inside the Open-ended L-shaped cavity with AR=0.4.
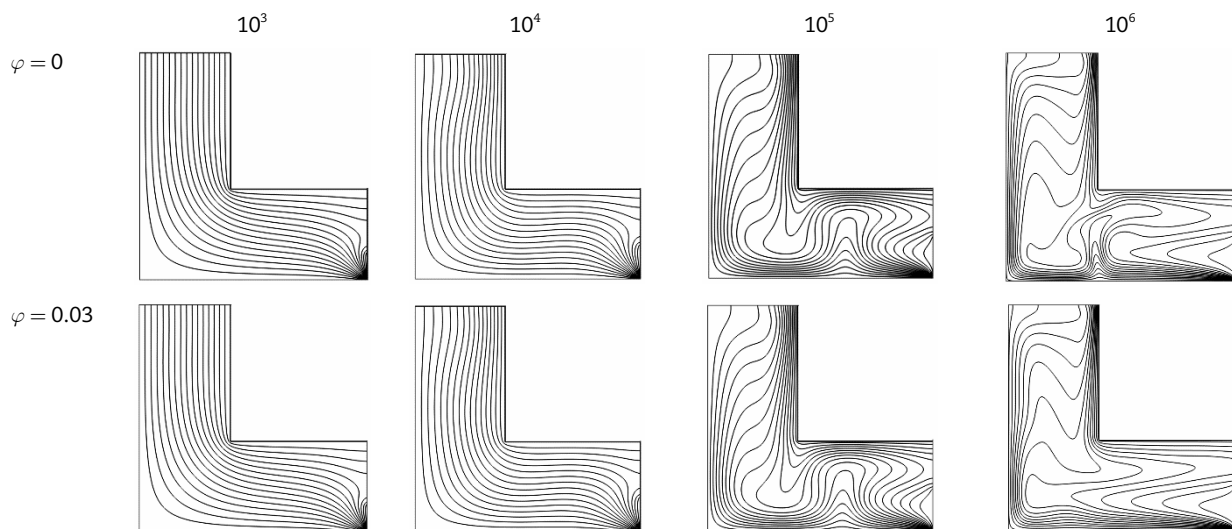

Fig. 12. Contour of the isotherms with volume fraction of the nanoparticles and Ra number for Cu/water nanofluid inside the Open-ended L-shaped cavity with AR=0.4.
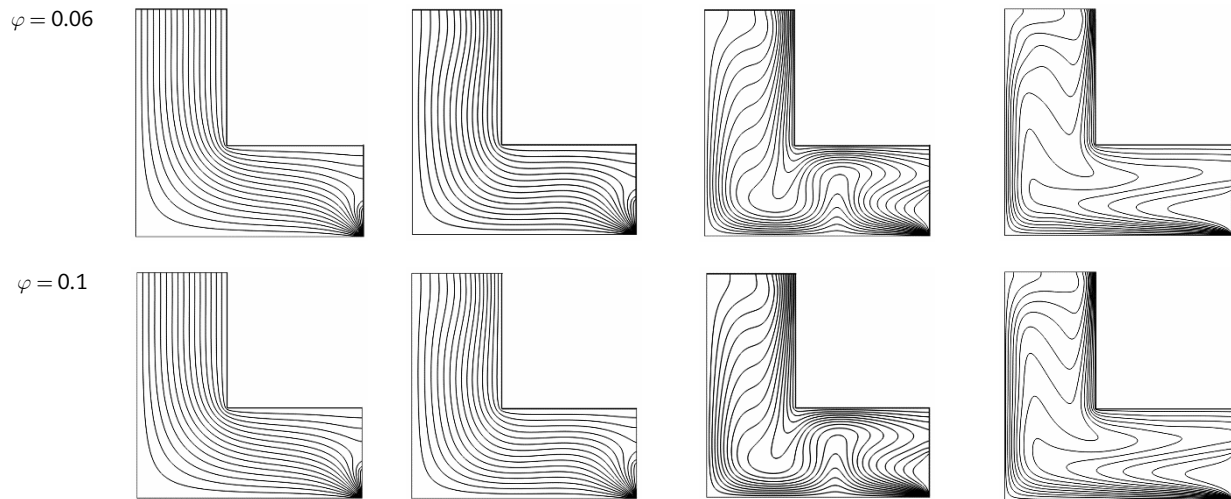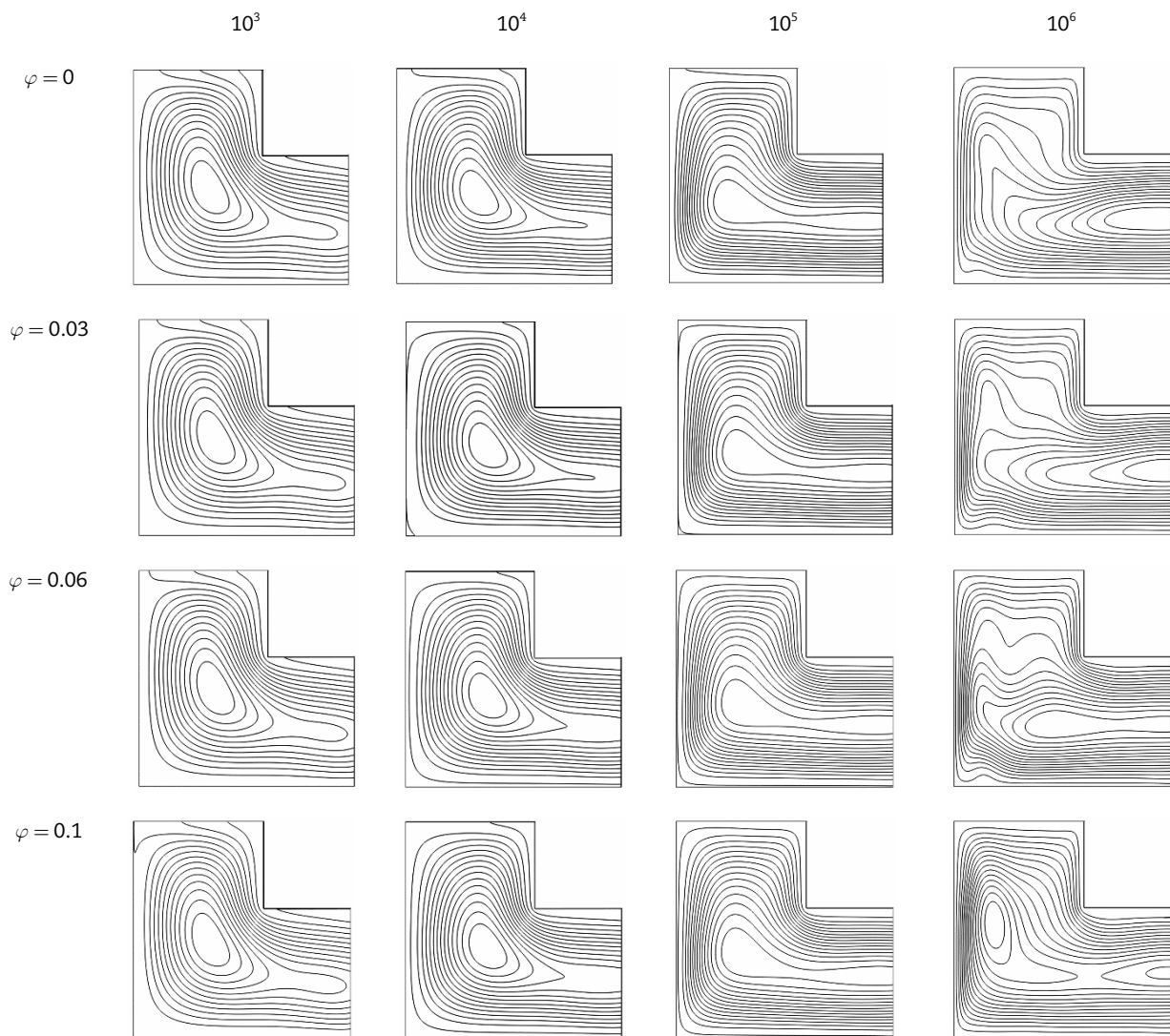
$\varphi = 0.06$

$\varphi = 0.1$

Fig. 12. Continued.

| | 10^3 | 10^4 | 10^5 | 10^6 |

$\varphi = 0$

$\varphi = 0.03$

$\varphi = 0.06$

$\varphi = 0.1$

Fig. 13. Contour of the streamlines with volume fraction of the nanoparticles and Ra number for Cu/water nanofluid inside the Open-ended L-shaped cavity with AR=0.6.
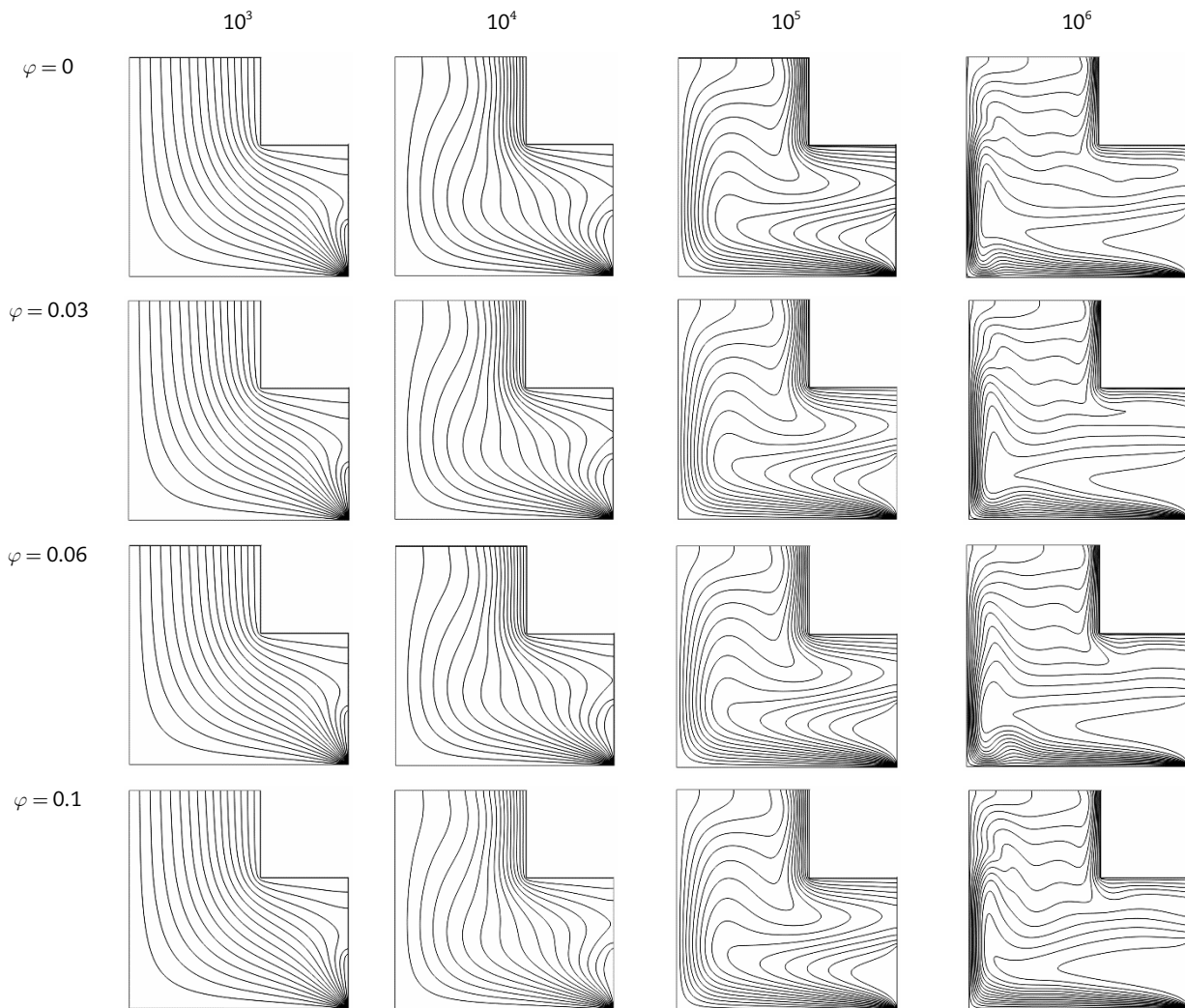
Fig. 14. Contour of the isotherms with volume fraction of the nanoparticles and Ra number for Cu/water nanofluid inside the Open-ended L-shaped cavity with AR=0.6.

Isotherms and streamlines for pure fluid and nanofluid natural convection in an open-ended L-shaped cavity for aspect ratio 0.4 at various Ra numbers are shown in Figs. 12 and 11 respectively. From Fig. 11 at Ra=10^3 and 10^4 for all volume concentration, exist a clockwise eddy in the vertical section of the L-shaped enclosure while; the flow in the horizontal part of the enclosure go down in near hot horizontal wall, and in open boundary part in the enclosure, isothermal condition go down to the hot horizontal wall. At Ra=10^5 in addition to existence a clockwise eddy in the vertical section, a counter clockwise eddy there is in the horizontal section of the enclosure. Finally, at Ra=10^6 the effect of the volume concentration of the nanoparticles on the streamlines is significant, so for pure fluid, there is a clockwise eddy and a counter clockwise eddy in the vertical and horizontal section of the enclosure respectively while for φ=0.03, 0.06 and 0.1 the streamlines extend to the entire L-shaped enclosure then cross into the open boundary. As it is clear in Fig. 12, isotherm lines for Ra=10^3 and Ra=10^4 are parallel with walls of the enclosure without considering the concentration of the nanoparticles. Also Fig. 12 shows the isotherm lines for Ra=10^5 are condensed close the walls and vertical oscillating in the vertical part and horizontal part of the L- shaped enclosure respectively which is indicative of changing the major heat transfer process from conduction to convective thermal flow. At Ra=10^6 the isotherm lines more intense accumulated towards close the wall in the vertical part of the enclosure and horizontal oscillating towards to the hot wall from open boundary region in the horizontal part of the enclosure. Therefore heat transfer characteristics augment by adding nanoparticles to water.

Figs. 13 and 14 show the isotherms and streamlines for open-ended L-shaped cavity with aspect ratio 0.6 and range of the concentration of the Cu nanoparticles 0≤ φ ≤0.1. Fig. 13 displays that for Ra=10^3 and 10^4 a clockwise eddy with diagonal elliptical core has appeared in the open-ended L-shaped enclosure for pure fluid and nanofluid while; the flow in close the open boundary enclosure go down in the near hot horizontal wall. With increasing the Ra from 10^3 to 10^5 for φ=0 and nanofluid with all the concentration of the Cu nanoparticles, a current eddy is disappeared gradually and crosses into the open boundary. At Ra=10^5 and 10^6, for φ=0, φ=0.03 and φ=0.06 eddy is gone and cross into the open boundary then again at φ=0.1 eddy to be formed. As it is clear in Fig. 14 isotherms at Ra=10^3 and Ra=10^4 with increment volume concentrations, does not change considerably and the main process of heat transfer is conduction. At Ra=10^5 the dominating heat transfer process is changed to convective thermal flow. Particularly at Ra=10^6 can be viewed as different thermal boundary layers are nearby the vertical walls that indicate the heat transfer process is free convection.

The effect of Rayleigh numbers and nanoparticle volume concentration on the mean Nusselt number for the hot walls has been shown in Fig. 15 for various aspect ratios. It is obvious that the mean Nusselt number enhancement rate by increment the volume concentration of Cu nanoparticles depends on the aspect ratio and Rayleigh number. Maximum and minimum the mean Nusselt number enhancement between base fluid (water) and Cu-H_2O nanofluid with φ=0.1 for Ra 10^6 with AR=0.4 (32.76%) and

AR=0.2 (28.68%) occurs respectively. From Fig. 15 it can be concluded that by increment Rayleigh number heat transfer increases for all values of the nanoparticle volume concentration and aspect ratios. Also, it was observed with increasing aspect ratios transition point from conduction to convective thermal flow happens in lower Rayleigh numbers.

It is obvious from Fig. 16 for Ra=10^3 and 10^4 with increasing aspect ratio, heat transfer rate reduces with respect to nanoparticles volume concentration, but at Ra=10^5 with increasing aspect ratio from 0.2 to 0.4 heat transfer rate enhances and then at aspect ratio 0.6 decreases. Therefore, the maximum rate of heat transfer is seen for AR=0.4. For Ra=10^6 with enhancement aspect ratio from 0.2 to 0.4 rate of heat transfer declines and then at cavity with AR=0.6 increases. Thus, it is obvious for the cavity with AR=0.4 minimum rate of heat transfer happens. It is observed that at Ra=10^3 and Ra=10^4, increment heat transfer rate by increasing nanoparticle volume concentration is higher for open-ended L-shaped enclosures with lower aspect ratio, but at Ra=10^5 and Ra=10^6 increasing heat transfer rate with an increment volume concentration of nanoparticles is almost equal for all aspect ratios. It can obvious from Fig. 16 that the maximum and minimum changes in mean Nusselt number enhancement for Ra=10^3 and Ra=10^5 by 76.6% and 2.28% when the aspect ratio of the cavity is decreased from AR=0.4 to AR=0.2 and AR=0.6 to AR=0.4, respectively.
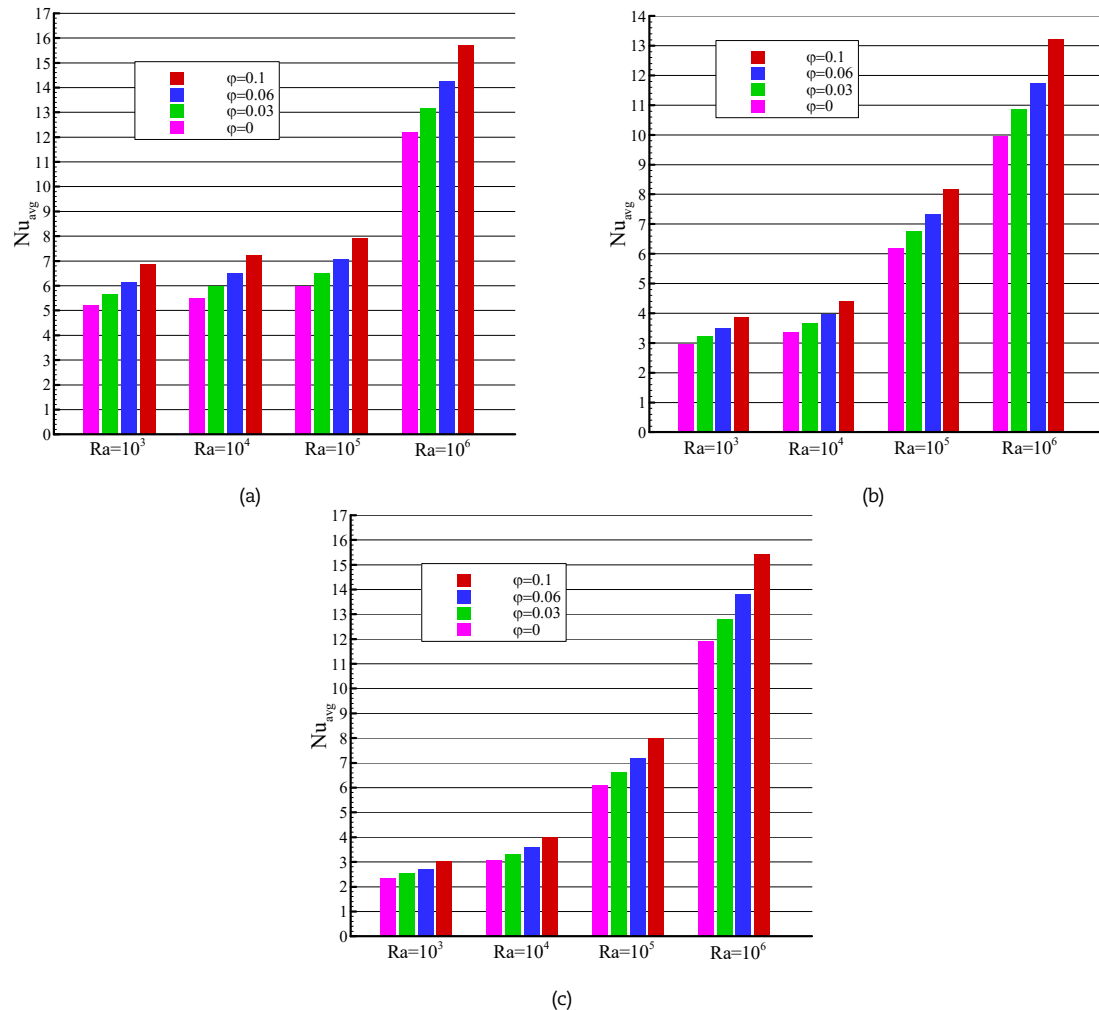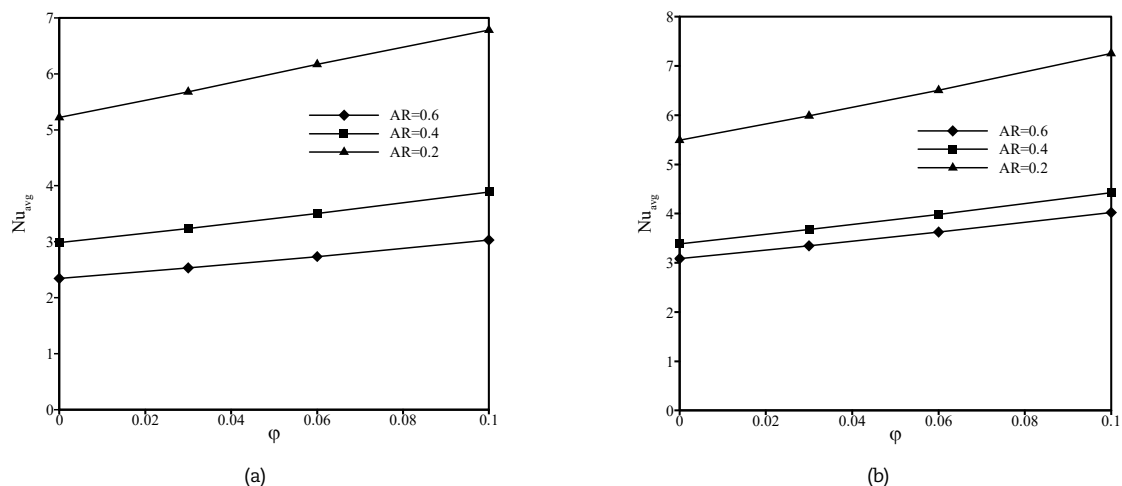

(a)

(b)

(c)

Fig. 15. Effect of nanoparticle volume concentration and Ra numbers on the average Nusselt number on the hot walls for (a) AR=0.2, (b) AR=0.4, (C) AR=0.6.
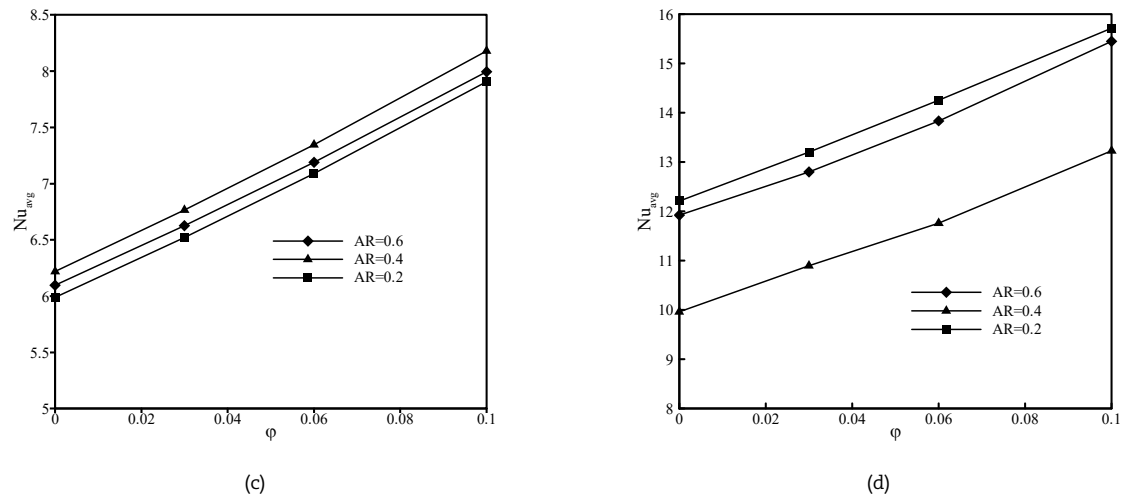

(a)

(b)

(c)   (d)

Fig. 16. Effect of nanoparticle volume concentration on the average Nusselt number on the hot walls for different aspect ratios with (a) $Ra=10^3$, (b) $Ra=10^4$, (C) $Ra=10^5$, (d) $Ra=10^6$.
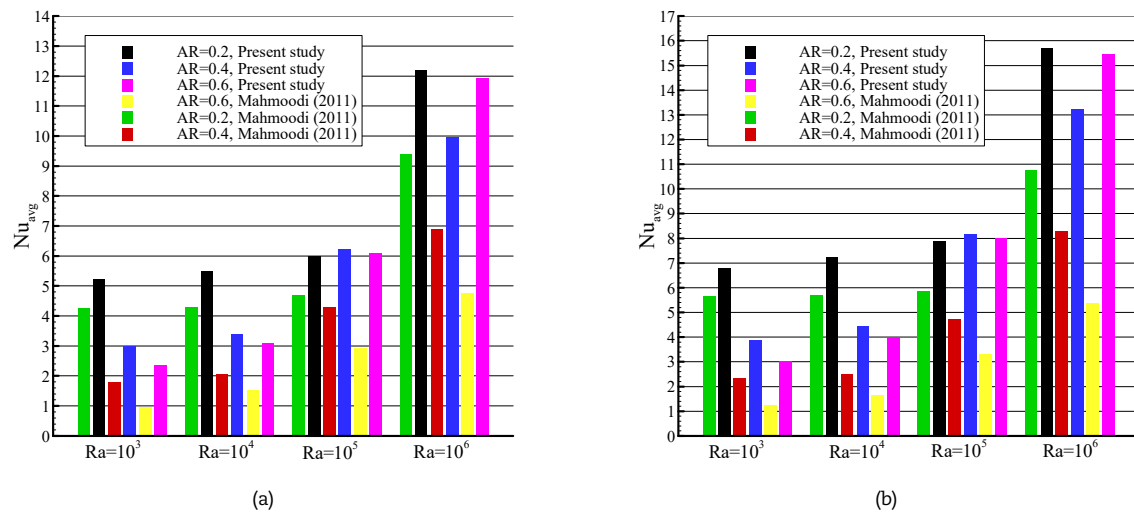

(a)   (b)

Fig. 17. Comparison of the average Nusselt number on the hot walls between the present study and Mostafa Mahmoodi [72], (Fig.6) (a) $\varphi=0$, (b) $\varphi=0.1$ for different Ra numbers and aspect ratios.

Table 4. Percentage of increase in the average Nusselt number for $\varphi=0$, $\varphi=0.1$, different Ra numbers and aspect ratios.

AR	Ra	ΔNu_f =Percentage of increase in the average Nusselt number by changing boundary conditions for pure fluid (water) $\varphi=0$	ΔNu_{nf} =Percentage of increase in the average Nusselt number by changing boundary conditions for nanofluid (Cu/H_2O) with $\varphi=0.1$	$\dfrac{\Delta Nu_{nf} - \Delta Nu_f}{\Delta Nu_f} \times 100$
AR=0.2	10^3	22.63%	21.57%	-4.68
	10^4	27.72%	27.12%	-2.16
	10^5	27.40%	35.39%	29.16
	10^6	29.87%	46.28%	54.93
AR=0.4	10^3	66.33%	65.04%	-1.94
	10^4	65.75%	77.39%	17.70
	10^5	44.63%	73.17%	63.94
	10^6	44.35%	59.63%	34.45
AR=0.6	10^3	143.36%	145.86%	1.74
	10^4	103.96%	144.41%	38.91
	10^5	107.55%	141.13%	31.22
	10^6	150.54%	186.92%	24.16

Fig. 18. Complex geometries for future studies in electronic cooling device

Fig. 17 demonstrates the effect of boundary conditions, by comparison, current work, and study of Mahmoodi [72], (Fig. 6) for base fluid (water) and Cu/H_2O nanofluid with φ=0.1. It is evident that the heat transfer enhanced for all values of the parameters considered when the boundary conditions have changed the end of the L-shaped cavity from the fixed wall with an adiabatic boundary condition to open boundary conditions. The maximum and minimum percentage increment average Nusselt number obtained for pure fluid (φ=0) by 150.54% and 22.63% for enclosure with AR=0.6 at Ra=10^6 and AR=0.2 at Ra=10^3, respectively. But for nanofluid (φ=0.1) maximum and minimum percentage enhancement average Nusselt number by 186.92% and 21.57% for the cavity with AR=0.6 at Ra=10^6 and AR=0.2 at Ra=10^3, respectively. So it can be concluded that the efficacy of changing the boundary conditions on increment the heat transfer is higher by increasing the aspect ratio from 0.2 to 0.6.

Table 4 shows the effect of changing boundary conditions on the rate of heat transfer, by calculation percentage of increases in the average Nusselt number between the present study, and Mahmoodi [72], (Fig. 6) for φ=0, φ=0.1 for different Ra numbers and aspect ratios. It is seen from Table 4. that for Ra numbers 10^3 and 10^4 with AR=0.2 and also Ra=10^3 with AR=0.4, the rate of increases heat transfer for the nanofluid is lower than for pure fluid when changing the boundary conditions, but for other cases, the opposite behavior can be seen. The greatest effect of changing boundary conditions and adding Cu nanoparticles to pure fluid (water) on increasing heat transfer is observed for the cavity aspect ratio 0.2, 0.4, and 0.6 in Ra numbers 10^6 (54.93%), 10^5 (63.94%), and 10^4 (38.91%) respectively. Therefore, the results of the present study can be used to increases cooling in order to the optimal design of various equipment in industries.

Finally, a correlation for the mean Nusselt number for each aspect ratio of open-ended L-shaped enclosure with variable parameters, Ra number, and the volume fraction of the nanoparticles was obtained as the following formula:

$$\begin{cases} Ra = 10^3 - 10^6 \\ \varphi = 0 - 0.1 \end{cases},$$

$$Nu_{avg} = \begin{cases} 5.28641 + 7.22803 \times 10^{-6} \times Ra + 1.68004 \times 10 \times \varphi + 1.83429 \times 10^{-5} \times Ra \times \varphi - 3.40128 \times 10^{-13} \times Ra^2, & AR = 0.2 \\ 2.83782 + 3.94551 \times 10^{-5} \times Ra + 1.20848 \times 10 \times \varphi + 2.08565 \times 10^{-5} \times Ra \times \varphi - 3.23962 \times 10^{-11} \times Ra^2, & AR = 0.4 \\ 2.32733 + 4.39332 \times 10^{-5} \times Ra + 1.06221 \times 10 \times \varphi + 2.52957 \times 10^{-5} \times Ra \times \varphi - 3.44669 \times 10^{-11} \times Ra^2, & AR = 0.6 \end{cases} \tag{33}$$

5. Conclusion

In this work, laminar natural convection thermal flow and heat transfer of Cu/H_2O nanofluid in open-ended L-shaped cavities were simulated by LBM. The effects of various important parameters like Rayleigh number, the volume concentration of the Cu nanoparticles, and various aspect ratios on the stream function, velocity, and heat transfer specifications have been studied and also, the effect of changing the boundary conditions, at the end of the L-shaped cavity on the heat transfer rate has been investigated and the following outcomes were achieved.

   i. The mean Nusselt number increases with raising Rayleigh number and volume concentration of the nanoparticles for all values of the aspect ratios.

   ii. The maximum effect of adding nanoparticles on increasing heat transfer for Ra=10^6 with AR=0.4 (32.76%) observed.

   iii. With increasing aspect ratios, the transition point from conduction to convection thermal flow happens in lower Rayleigh numbers.

   iv. At Ra=10^3 and 10^4 with increasing aspect ratio, the rate of heat transfer reduces regardless of the concentration of the nanoparticles. Moreover at Ra=10^5 cavity with AR=0.2 and AR=0.4 minimum and maximum rate of heat transfer occur respectively, But at Ra=10^6 cavity with aspect ratios of 0.4 and 0.2 minimum and maximum rate of heat transfer happens respectively.

   v. The maximum changes in heat transfer enhancement in Ra=10^3 by 76.6% with decreasing the aspect ratio of the cavity from 0.4 to 0.2 occur.

   vi. The heat transfer enhanced (maximum 186.92%) for all values of the parameters considered when the boundary conditions have changed the end of the L-shaped cavity from the fixed wall with an adiabatic boundary condition to open boundary conditions.

6. Future work

Some suggestions for the future studies can be considered as follows:

i. Investigation of free convection heat transfer in other geometries with more complex patterns and curved corners (Fig. 18) and using fins in internal and external sections in order to increase the cooling efficiency in various industries, especially electronic cooling equipment.

ii. Investigation of different types of single and hybrids nanoparticles and various base fluids for nanofluid.

iii. To consider new nanofluid models and new experimental models to obtain the thermophysical properties of nanofluid.

iv. Examination of the effect of the magnetic field and porous media on fluid flow and heat transfer.

v. To consider different boundary conditions for walls such as; constant and variable thermal flux, variable temperature distribution.

vi. Three-dimensional natural convection simulation using dual multiple relaxation time lattice Boltzmann method in the curve and asymmetric geometries.

Conflict of Interest

The authors declared no potential conflicts of interest with respect to the research, authorship and publication of this article.

Funding

Nomenclature

AR	Aspect ratio AR=D/Z	U,V	Dimensionless velocities components in X and Y direction
c	Lattice speed	u,v	Dimensional velocities components in x and y direction [m/s]
c_i	Discrete particle speeds	α	Thermal diffusivity $[m^2/s]$
c_p	Specific heat in constant pressure [kJ/kg k]	β	Thermal expansion coefficient (1/K)
f	Density distribution functions	θ	Dimensionless temperature
f^{eq}	Equilibrium density distribution functions	ϕ	Volume fraction of the nanoparticles
g	Internal energy distribution functions	τ_c	Relaxation time for temperature
g^{eq}	Equilibrium internal energy distribution functions	τ_v	Relaxation time for flow
g_y	Gravity $[m/s^2]$	μ	Dynamic viscosity [kg/ms]
h	Heat transfer coefficient $[WK/m^2]$	ϑ	Kinematic viscosity $[m^2/s]$
Z	Enclosure height and width [m]	ρ	Density $[kg/m^3]$
K	Thermal conductivity [w/mk]		
Nu	Nusselt number		**Subscripts**
Pr	Prandtl number Pr=ϑ/α	avg	average
q	Heat flux $[W/m^2]$	c	cold
Ra	Rayleigh number $Ra = (\beta g_y Z^3 (T_h - T_c))/\vartheta\alpha$	f	fluid
T	Temperature [K]	h	hot
x,y	Cartesian coordinates	nf	nanofluid
X,Y	Dimensionless Cartesian coordinates	s	solid particles
		l	Local

References

[1] Khanafer, Kh.M. and Chamkha, A.J., Hydromagnetic Natural Convection from an Inclined Porous Square Enclosure with Heat Generation, *Numerical Heat Transfer, Part A: Applications*, 33(8), 1998, 891-910.

[2] Kim, B.S., Lee, B.I., Lee, N., Choi, G., Gemming, T., Cho, H.H., Nano-inspired smart interfaces: fluidic interactivity and its impact on heat transfer, *Scientific Reports*, 7, 2017, 45323.

[3] Khan, I. and Shah, N.A., A scientific report on heat transfer analysis in mixed convection flow of Maxwell fluid over an oscillating vertical plate, *Scientific Reports*, 7, 2017, 40147.

[4] Thippeswamy, L.R. and Yadav, A.K., Heat transfer enhancement using CO_2 in a natural circulation loop, *Scientific Reports*, 10, 2020, 1507.

[5] Fattahi, E., Farhadi, M., Sedighi, K., Lattice Boltzmann simulation of natural convection heat transfer in eccentric annulus, *International Journal of Thermal Sciences*, 49, 2010, 2353-2362.

[6] Nemati, H., Farhadi, M., Sedighi, K., Fattahi, E., Rabienataj, A.A., Lattice Boltzmann simulation of nanofluid in lid-driven cavity, *International Communications in Heat and Mass Transfer*, 37, 2010, 1528-1534.

[7] Kefayati, G.H.R., Hosseinizadeh, S.F., Gorji, M., Sajjadi, H., Lattice Boltzmann simulation of natural convection in tall enclosures using water/SiO_2 nanofluid, *International Communications in Heat and Mass Transfer*, 38, 2011, 798-805.

[8] Nemati, H., Farhadi, M., Sedighi, K., Ashorynejad, H.R., Fattahi, E., Magnetic field effects on natural convection thermal flow of nanofluid in a rectangular cavity using the Lattice Boltzmann model, *Scientia Iranica*, 19(2), 2012, 303–310.

[9] Jourabian, M., Farhadi, M., Rabienataj Darzi, A.A., Simulation of natural convection melting in an inclined cavity using lattice Boltzmann method, *Scientia Iranica*, 19(4), 2012, 1066–1073.

[10] Jin, L., Zhang, X., Niu, X., Lattice Boltzmann simulation for temperature-sensitive magnetic fluids in a porous square cavity, *Journal of Magnetism and Magnetic Materials*, 324, 2012, 44-51.

[11] Nazari, M., Kayhani, M.H., A Comparative Solution of Natural Convection in an Open Cavity using Different Boundary Conditions via the Lattice Boltzmann Method, *Journal of Heat and Mass Transfer Research*, 3, 2016, 115-129.

[12] Ahmed, M., Eslamian, M., Natural convection in a differentially-heated square enclosure filled with a nanofluid: Significance of the thermophoresis force and slip/drift velocity, *International Communications in Heat and Mass Transfer*, 58, 2014, 1–11.

[13] Sajjadi, H., Salmanzadeh, M., Ahmadi, G., Jafari, S., Investigation of particle deposition and dispersion using Hybrid LES/RANS model based on Lattice Boltzmann method, *Scientia Iranica*, 25, 2018, 3173-3182.

[14] Jalali, A., Delouei, A.A., Khorashadizadeh, M., Golmohammadi, A.M., Karimnejad, S., mesoscopic simulation of forced convective heat transfer of carreau-yasuda fluid flow over an inclined square: temperature-dependent viscosity, *Journal of Applied and Computational Mechanics*, 6(2), 2020, 307-319.

[15] Choi, U.S., Enhancing thermal conductivity of fluids with nanoparticles, developments and application of non-Newtonian flows, *ASME*, 66, 1995, 99-105.

[16] Hashim, Hafeez, A., Alshomrani, A.S., Khan, M., Multiple physical aspects during the flow and heat transfer analysis of Carreau fluid with nanoparticles, *Scientific Reports*, 8, 2018, 17402.

[17] Carrillo-Berdugo, I., Zorrilla, D., sanchez-Marquez, J., Aguilar, t., Gallardo, J.J., Gomez-Villarejo, R., Alcantara, R., Fernandez-Lorenzo, C., Navas, J., Interface-inspired formulation and molecular-level perspectives on heat conduction and energy storage of nanofluids, *Scientific Reports*, 9, 2019, 7595.

[18] Sheikholeslami, M., Sajjadi, H., Delouei, A.A, Atashafrooz, M., Li, Zh., Magnetic force and radiation influences on nanofluid transportation through a permeable media considering Al_2O_3 nanoparticles, *Journal of Thermal Analysis and Calorimetry*, 136, 2019 ,2477–2485.

[19] Chamkha, A.J., Molana, M., Rahnama, A., Ghadami F., On the nanofluids applications in microchannels: A comprehensive review, *Powder Technology*, 332, 2018, 287-322.

[20] Chamkha, A.J., Rashad, A.M., Mansour, M.A., Armaghani, T., Ghalambaz, M., Effects of heat sink and source and entropy generation on MHD mixed convection of a Cu-water nanofluid in a lid-driven square porous enclosure with partial slip, *Physics of Fluids*, 29, 2017, 052001-22.

[21] Rashad, A.M., Armaghani, T., Chamkha, A.J., Mansour, M.A., Entropy Generation and MHD Natural Convection of a Nanofluid in an Inclined Square Porous Cavity: Effects of a Heat Sink and Source Size and Location, *Chinese Journal of Physics*, 56(1), 2018, 193-211.

[22] Khanafer, K., Vafai, K., Lightstone, M., Buoyancy-driven heat transfer enhancement in a two dimensional enclosure utilizing nanofluid, *International Journal of Heat and Mass Transfer*, 46, 2003, 3639-3653.

[23] Lai, F.H., Yang, Y.T., Lattice Boltzmann simulation of natural convection heat transfer of Al_2O_3/water nanofluids in a square enclosure, *International Journal of Thermal Sciences*, 50, 2011, 1930-1941.

[24] Fattahi, E., Farhadi, M., Sedighi, K., Nemati, H., Lattice Boltzmann simulation of natural convection heat transfer in nanofluids, *International Journal of Thermal Sciences*, 52, 2012, 137-144.

[25] Kefayati, GH.R., Effect of a magnetic field on natural convection in an open cavity subjugated to water/alumina nanofluid using Lattice Boltzmann method, *International Communications in Heat and Mass Transfer*, 40, 2013, 67–77.

[26] Oztop, H.F., Abu-Nada, E., Numerical study of natural convection in partially heated rectangular enclosures filled with nanofluids, *International Journal of Heat and Fluid Flow*, 29, 2008, 1326-1336.

[27] Jahanshahi, M., Hosseinizadeh, S.F., Alipanah, M., Dehghani, A., Vakilinejad G.R., Numerical simulation of free convection based on experimental measured conductivity in a square cavity using water/SiO_2 nanofluid, *International Communications in Heat and Mass Transfer*, 37, 2010, 687-694.

[28] Mahmoudi, A.H., Shahi, M., Shahedin, A.M., Hemati, N., Numerical modeling of natural convection in an open enclosure with two vertical thin heat sources subjected to a nanofluid, *International Communications in Heat and Mass Transfer*, 38, 2011,110-118.

[29] Kefayati, G.H.R., Hosseinizadeh, S.F., Gorji, M., Sajjadi, H., Lattice Boltzmann simulation of natural convection in an open enclosure subjugated to water/copper nanofluid, *International Journal of Thermal Sciences*, 52, 2012, 91-101.

[30] Shahriari, A.R., Jafari, S., Rahnama, M., Behzadmehr, A., Effect of nanofluid variable properties on natural convection in a square cavity using Lattice Boltzmann method, *International Review of Mechanical Engineering*, 7, 2013, 442–452.

[31] Hu, Y., He, Y., Qi, C., Jiang, B., Schlaberg, H.I., Experimental and numerical study of natural convection in a square enclosure filled with nanofluid, *International Journal of Heat and Mass Transfer*, 78, 2014, 380-392.

[32] Zhou, W.N., Yan, Y.Y., Xu, J.L., A lattice Boltzmann simulation of enhanced heat transfer of nanofluids, *International Communications in Heat and Mass Transfer*, 55, 2014, 113-120.

[33] Hosseini, M., Mustafa, M.T., Jafaryar, M., Mohammadian, E., Nanofluid in tilted cavity with partially heated walls, *Journal of Molecular Liquids*, 199, 2014, 545-551.

[34] Jafari, M., Farhadi, M., Akbarzade, S., Ebrahimi, M., Lattice Boltzmann simulation of natural convection heat transfer of SWCNT-nanofluid in an open enclosure, *Ain Shams Engineering Journal*, 6(3), 2015, 913-927.

[35] Sheikholeslami, M., Ashorynejad, H.R., Rana, P., Lattice Boltzmann simulation of nanofluid heat transfer enhancement and entropy generation, *Journal of Molecular Liquids*, 214, 2016, 86-95.

[36] Sajjadi, H., Delouei, A.A., Izadi, M., Mohebbi, R., Investigation of MHD natural convection in a porous media by double MRT lattice Boltzmann method utilizing MWCNT–Fe_3O_4/water hybrid nanofluid, *International Journal of Heat and Mass Transfer*, 132, 2019, 1087-1104.

[37] Sajjadi, H., Amiri Delouei, A., Atashafrooz, M., Sheikholeslami, M., Double MRT Lattice Boltzmann simulation of 3-D MHD natural convection in a cubic cavity with sinusoidal temperature distribution utilizing nanofluid, *International Journal of Heat and Mass Transfer*, 126, 2018, 489–503.

[38] Rahimi, A., Kasaeipoor, A., Malekshah, E.H., kolsi, L., Natural convection analysis by entropy generation and heatline visualization using lattice Boltzmann method in nanofluid filled cavity included with internal heaters- Empirical thermo-physical properties, *Journal of Molecular Liquids*, 133, 2017, 199-216.

[39] Rahimi, A., Kasaeipoor, A., Malekshah, E.H., Lattice Boltzmann simulation of natural convection and entropy generation in cavities filled with nanofluid in existence of internal rigid bodies-Experimental thermo-physical properties, *Journal of Molecular Liquids*, 242, 2017, 580-593.

[40] Mehrizi, A., Farhadi, M., Shayamehr, S., Natural convection flow of Cu–Water nanofluid in horizontal cylindrical annuli with inner triangular cylinder using lattice Boltzmann method, *International Communications in Heat and Mass Transfer*, 44, 2013, 147-156.

[41] Abdallaoui, M.El., Hasnaoui, M., Amahmid, A., Numerical simulation of natural convection between a decentered triangular heating cylinder and a square outer cylinder filled with a pure fluid or a nanofluid using the lattice Boltzmann method, *Powder Technology*, 277, 2015, 193–205.

[42] Hatami, M., Numerical study of nanofluids natural convection in a rectangular cavity including heated fins, *Journal of Molecular Liquids*, 233, 2017, 1-8.

[43] Torabi, M., Keyhani, A.R., Peterson, G.P., A comprehensive investigation of natural convection inside a partially differentially heated cavity with a thin fin using two-set lattice Boltzmann distribution functions, *International Journal of Heat and Mass Transfer*, 115, 2017, 264-277.

[44] Chamkha, A.J., Doostanidezfuli, A., Izadpanahi, E., Ghalambaz, M., Phase-change heat transfer of single/hybrid nanoparticles-enhanced phase-change materials over a heated horizontal cylinder confined in a square cavity, *Advanced Powder Technology*, 28(2), 2017, 385-397.

[45] Pordanjani, A.H., Jahanbakhshi, A., Nadooshan, A.A., Afrand, M., Effect of two isothermal obstacles on the natural convection of nanofluid in the presence of magnetic field inside an enclosure with sinusoidal wall temperature distribution, *International Journal of Heat and Mass Transfer*, 121, 2018, 565–578.

[46] Siavashi, M., Yousofvand, R., Rezanejad, S., Nanofluid and porous fins effect on natural convection and entropy generation of flow inside a cavity, *Advanced Powder Technology*, 29, 2018, 142-156.

[47] Vijaybabu, T.R., Dhinakaran, S., MHD Natural convection around a permeable triangular cylinder inside a square enclosure filled with Al_2O_3-H_2O nanofluid: An LBM study, *International Journal of Mechanical Sciences*, 153–154, 2019, 500-516.

[48] Hashim, I., Alsabery, A.I., Sheremet, M.A., Chamkha, A.J., Numerical investigation of natural convection of -water nanofluid in a wavy cavity with conductive inner block using Buongiorno's two-phase model, *Advanced Powder Technology*, 30, 2019, 399-414.

[49] Dindarloo, M.R., Payan, S., Effect of fin thickness, grooves depth, and fin attachment angle to the hot wall on maximum heat transfer reduction in a square enclosure, *International Journal of Thermal Sciences*, 136, 2019, 473–490.

[50] Koca, A., Oztop, H.F., Varol, Y., Numerical analysis of natural convection in shed roofs with eave of buildings for cold climates, *Computers & Mathematics with Applications*, 56, 2008, 3165-3174.

[51] Dehnavi, R., Rezvani, A., Numerical investigation of natural convection heat transfer of nanofluids in a ⌀ shaped cavity, *Superlattices and Microstructures*, 52, 2012, 312–325.

[52] Kalteh, M., Hasani, H., Lattice Boltzmann simulation of nanofluid free convection heat transfer in an L-shaped enclosure, *Superlattices and Microstructures*, 66, 2014, 112-128.

[53] Parvin, S., Nasrin, R., Alima, M.A., Hossain, N.F., Chamkha, A.J., Thermal conductivity variation on natural convection flow of water–alumina nanofluid in an annulus, *International Journal of Heat and Mass Transfer*, 55, 2012, 5268–5274.

[54] Gallegos, A.D., Malaga, C., Natural convection in eccentric spherical annuli, *European Journal of Mechanics - B/Fluids*, 65, 2017, 464-471.

[55] Parvin, S., Nasrin, R., Alim, M.A., Hossain, N.F., Chamkha, A.J., Thermal conductivity variation on natural convection flow of water–alumina nanofluid in an annulus, *International Journal of Heat and Mass Transfer*, 55, 2012, 5268–5274.

[56] Sheikholeslami, M., Gorji-Bandpy, M., Seyyedi, S.M., Ganji, D.D., Rokni, H.B., Soleimani, S., Application of LBM in simulation of natural convection

in a nanofluid filled square cavity with curve boundaries, *Powder Technology*, 247, 2013, 87–94.

[57] Ghadi, A.Z., Haghighi Asl, A., Valipour, M.S., Numerical modelling of double-diffusive natural convection within an arc-shaped enclosure filled with a porous medium, *Journal of Heat and Mass Transfer Research*, 1, 2014, 83-91.

[58] Jayhooni, S.M.H., Jafarpur, K., Numerical simulation of Laminar Free Convection Heat Transfer around Isothermal Concave and Convex Body Shapes, *Journal of Heat and Mass Transfer Research*, 2, 2015, 37-44.

[59] Rezvani, A., Valipour, M.S., Biglari, M., Numerical Study of Entropy Generation for Natural Convection in Cylindrical Cavities, *Journal of Heat and Mass Transfer Research*, 3 (2016) 89-99.

[60] Ghasemi, B., Aminossadati, S.M., Brownian motion of nanoparticles in a triangular enclosure with natural convection, *International Journal of Thermal Sciences*, 49, 2010, 931-940.

[61] Saleh, H., Roslan, R., Hashim, I., Natural convection heat transfer in a nanofluid filled trapezoidal enclosure, *International Journal of Heat and Mass Transfer*, 54, 2011, 194-201.

[62] Mejri, I., Mahmoudi, A., Abbassi, M.A., Omri, A., LBM simulation of natural convection in an inclined triangular cavity filled with water, *Alexandria Engineering Journal*, 55(2), 2016, 1385-1394.

[63] Chamkha, A.J., Ismael, M., Kasaeipoor, A., Armaghani, T., Entropy Generation and Natural Convection of CuO-Water Nanofluid in C-Shaped Cavity under Magnetic Field, *Entropy*, 18(2), 2016, 50.

[64] Mohebbi, R., Izadi, M., Chamkha, A.J., Heat source location and natural convection in a C-shaped enclosure saturated by a nanofluid, *Physics of Fluids*, 29, 2017, 122009-13.

[65] Bondareva, N.S., Sheremet, M.A., Oztop, H.F., Abu-Hamdeh, N., Entropy generation due to natural convection of a nanofluid in a partially open triangular cavity, *Advanced Powder Technology*, 28(1), 2017, 244-255.

[66] Mahmoodi, M., Hashemi, S.M., Numerical study of natural convection of a nanofluid in C-shaped enclosures, *International Journal of Thermal Sciences*, 55, 2012, 76-89.

[67] Mansour, M.A., Bakier, A.Y., Bakier, M.A.Y., Natural convection of the localized heat sources of T-shaped nanofluid filled enclosures, *American Journal of Engineering Research*, 2(7) , 2013, 49-61.

[68] Bakier, M.A.Y., Flow in open C-shaped cavities: How far does the change in boundaries affect nanofluid?, *Engineering Science and Technology, an International Journal*, 17, 2014, 116-130.

[69] Esfea, M.H., Abbasian Arani, A.A., Yanc, W.M., Aghaei, A., Natural convection in T-shaped cavities filled with water-based suspensions of COOH-functionalized multi walled carbon nanotubes, *International Journal of Mechanical Sciences*, 121, 2017, 21–32.

[70] Mahmud, S., Free convection inside an L-shaped enclosure, *International Communications in Heat and Mass Transfer*, 29, 2002, 1005-1013.

[71] Tasnim, S.H., Mahmud, S., Laminar free convection inside an inclined L-shaped enclosure, *International Communications in Heat and Mass Transfer*, 33, 2006, 936-942.

[72] Mahmoodi, M., Numerical simulation of free convection of a nanofluid in L-shaped cavities, *International Journal of Thermal Sciences*, 50, 2011, 1731-1740.

[73] Sheikholeslami, M., Gorji-Bandpy, M., Ganji, D.D., Soleimani, S., Natural convection heat transfer in a nanofluid filled inclined L-shaped enclosure, *Iranian Journal of Science and Technology, Transactions of Mechanical Engineering*, 38, 2014, 217-226.

[74] Mliki, B., Abbassi, M.A., Guedri, K., Omri, A., Lattice Boltzmann simulation of natural convection in an L-shaped enclosure in the presence of nanofluid, *Engineering Science and Technology an International Journal*, 18, 2015, 503-511.

[75] Mohebbi, R., Rashidi, M.M., Numerical simulation of natural convection heat transfer of a nanofluid in an L-shaped enclosure with a heating obstacle, *Journal of the Taiwan Institute of Chemical Engineers*, 72, 2017, 70-84.

[76] Rahimi, A., Kasaeipoor, A., Malekshah, E.H., Amiri, A., Natural convection analysis employing entropy generation and heatline visualization in a hollow L-shaped cavity filled with nanofluid using lattice Boltzmann method- experimental thermo-physical properties, *Physica E: Low-dimensional Systems and Nanostructures*, 97, 2018, 82-97.

[77] Zhang, R., Aghakhani, S., Hajatzadeh Pordanjani, A. et al., Investigation of the entropy generation during natural convection of Newtonian and non-Newtonian fluids inside the L-shaped cavity subjected to magnetic field: application of lattice Boltzmann method, *The European Physical Journal Plus*, 135, 2020, 184.

[78] Izadi, M., Mohebbi, R., Delouei, A.A., Sajjadi, H., Natural convection of a magnetizable hybrid nanofluid inside a porous enclosure subjected to two variable magnetic fields, *International Journal of Mechanical Sciences*, 151, 2019, 154-169.

[79] Abbassi, M.A., Safaei, M.R., Djebali, R., Guedri, K., Zeghmati, B., Alrashedg, A. A.A.A., LBM simulation of free convection in a nanofluid filled incinerator containing a hot block, *International Journal of Mechanical Sciences*, 148, 2018, 393-408.

[80] Ma, Y., Mohebbi, R., Rashidi, M.M., Yang, Zh., Simulation of nanofluid natural convection in a U-shaped cavity equipped by a heating obstacle: Effect of cavity's aspect ratio, *Journal of the Taiwan Institute of Chemical Engineers*, 93, 2018, 263-276.

[81] Y.M. Seo, M. Yeong Ha, Y. Gap Park, A numerical study on the three-dimensional natural convection with a cylinder in a long rectangular enclosure. Part I: Size effect of a circular cylinder or an elliptical cylinder, *International Journal of Heat and Mass Transfer*, 134, 2019, 420-436.

[82] Dutta, S., Goswami, N., Biswas, A.K., Pati, S., Numerical investigation of magnetohydrodynamic natural convection heat transfer and entropy generation in a rhombic enclosure filled with Cu-water nanofluid, *International Journal of Heat and Mass Transfer*, 136, 2019, 777–798.

[83] Purusothaman, A., Malekshah, E.H., Lattice Boltzmann modeling of MHD free convection of nanofluid in a V-shaped microelectronic module, *Thermal Science and Engineering Progress*, 10, 2019, 186-197.

[84] Yahiaoui, A., Djezzar, M., Naji, H., Simulating of heat transfer enhancement via a water-based nanofluid in enclosures with curved side walls, *International Communications in Heat and Mass Transfer*, 100, 2019, 118–132.

[85] Almeshaal, M.A, Maatki, C., Kolsi, L., Ghachem, K., Chamkha, A.J., 3D Rayleigh-Bénard-type natural convection in MWCNT-nanofluid-filled L-shaped enclosures with consideration of aggregation effect, *Mathematical Methods in the Applied Sciences*, 2020, 1–17.

[86] Dogonchi, A.S., Chamkha, A.J., Seyyedi, S.M., Hashemi-Tilehnoee, M., Ganji, D.D., Viscous dissipation impact on free convection flow of Cu-water nanofluid in a circular enclosure with porosity considering internal heat source, *Journal of Applied and Computational Mechanics*, 5(4), 2019, 717-726.

[87] Bejan, A., *Convection Heat Transfer*, John Wiley & Sons, Inc., Hoboken, New Jersey, USA, 2004.

[88] Mohamad, A.A., Kuzmin, A., A critical evaluation of force term in lattice Boltzmann method, natural convection problem, *International Journal of Heat and Mass Transfer*, 53, 2010, 990-996.

[89] Mohamad, A.A., El-Ganaoui, M., Bennacer, R., Lattice Boltzmann simulation of natural convection in an open ended enclosure, *International Journal of Thermal Sciences*, 48, 2009, 1870-1875.

[90] Wang, X.Q., Mujumdar, A.S., Heat transfer characteristics of nanofluids: a review, *International Journal of Thermal Sciences*, 46(1), 2007, 1-19.

[91] Hwang, K.S., Lee, J.H., Jang, S.P., Buoyancy-driven heat transfer of water-based Al_2O_3 nanofluids in a rectangular enclosure, *International Journal of Heat and Mass Transfer*, 50(19-20), 2007, 4003-4010.

[92] Mohamad, A.A., Natural convection in open cavities and slots, *Numerical Heat Transfer, Part A: Applications*, 27, 1995, 705-716.

ORCID iD

Hasan Mohammadifar https://orcid.org/0000-0003-0704-9395

Hasan Sajjadi https://orcid.org/0000-0002-0681-7682

Mohammad Rahnama https://orcid.org/0000-0003-3569-8704

Saeed Jafari https://orcid.org/0000-000x-xxxx-xxxx

Yan Wang https://orcid.org/0000-0002-4352-1450

Publisher's Note Shahid Chamran University of Ahvaz remains neutral with regard to jurisdictional claims in published maps and institutional affiliations.